

## Introduction

It is crucial that fluorescent biosensors are selective so that they demonstrate diagnostic signals which corresponds to the presence of the target molecule. A distinct difference between the signal when a non-target molecule is introduced compared to the signal when the target analyte is essential. In addition to selectivity, a biosensor must also be sensitive. Low concentrations of analyte limit the identification of the target as well as the accuracy. For these reasons, signal amplification schemes provide improved sensitivity. Conjugated polymers (CPs) contain characteristics that overcome previous limitations by analytical techniques, such as ELISA. CPs can be optimized for optical amplification using exciton mobility. The overall sensitivity of the CPs depend on the analyte specific interactions with the side chains and structure of the CP<sup>1</sup>.

The importance of water solubility is fundamental for biosensors. CPs can be synthesized to incorporate charged side groups to the polymer's backbone to help it dissolve in aqueous

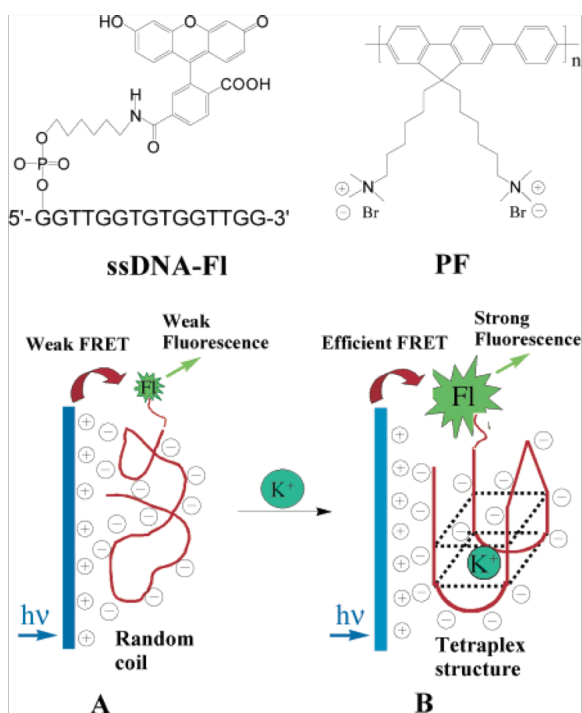


Figure 1. The structures fluorescein labeled ssDNA and CP (PF) are shown. A demonstrates a weak FRET when  $K^+$  is not present as compared to the high FRET situation when the ssDNA adopts a quadruplex conformation in the presence of  $K^+$ .

solutions. However, non-aggregated CPs that are water soluble are difficult to form due to their high aromatic components on the backbone chain. Nonetheless, the potential of using CPs as a biosensor allows for amplified analysis and can be modified in order to increase specificity. This amplification occurs through electronic excited states, called excitons, which are mobile throughout the conjugated pi system of the polymer<sup>2</sup>. Furthermore, the excited states of CPs can be quenched through a quencher that is bound to the receptor or in close proximity. The mobility of the excitons and charges allows for high sensitivity in the CPs. Variations of conjugated polymers, such as electrostatic or hydrophobic components, can allow for specific control of analyte detection.

Conjugated polymers also have the advantages in that they allow for tunable adjustments to be made through their physical properties such as color and fluorescence.

An example of these CPs detecting various analytes includes the detection of potassium ions. The use of a ssDNA with a water soluble cationic poly(thiophene) complex was responsive to potassium ions<sup>3</sup>. The 5' fluorescein labeled ssDNA possesses the ability to fold into G-quadruplexes due to its hydrogen bonding by its G-rich sequence (Figure 1). However, the

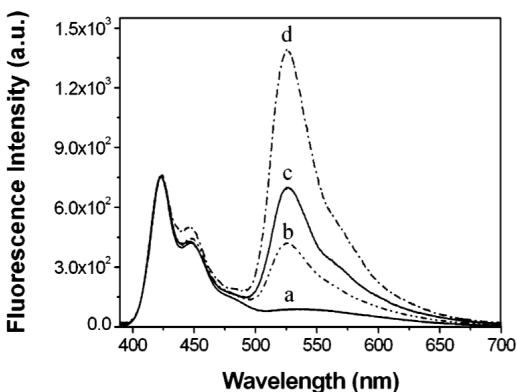


Figure 2. The fluorescence of the CP increased with increasing concentrations of  $K^+$ , from a to d.

ssDNA only adopts this structure in the presence of potassium ions. The addition of potassium ions increases the space charge density around the DNA molecule, inducing the formation of a condensed secondary structure. The emission of the CP, poly(9,9-bis(6'-N,N,N-trimethylammonium)hexyl)fluorenylene

phenylene, overlaps greatly with the absorption of the fluorophore on the ssDNA, allowing for potentially efficient FRET. Potassium ion addition shifted the uncoiled ssDNA to a quadruplex

structure, decreasing the distance between the PF donor and the acceptor. In a weak FRET situation, the random coil has weak electrostatic interactions with the CP and the fluorophore on the DNA is kept far away. In the presence of potassium ions, a quadruplex structure is formed, which gives a high FRET scenario. As the concentration of potassium ions increase, the fluorescence of the CP increases as well (Figure 2). Other cations were similarly analyzed, though sodium, lithium, and ammonium ions did not result in inducing a G-quadruplex, and therefore had weak FRET (Figure 3). The FRET ratio was nearly 16 times higher for potassium ions than that of various cations. Different polymers have also been developed to detect lithium and sodium ions, as well as  $Eu^{3+}$ ,  $Cu^{2+}$ ,  $Co^{2+}$ , and  $Fe^{3+}$ .<sup>2</sup> The last three were detectable through the

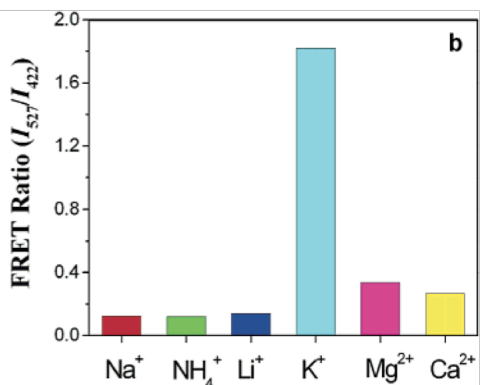


Figure 3. The quadruplex structure of the ssDNA is induced in the presence of  $K^+$ , allowing for efficient FRET.

which gives a high FRET scenario. As the concentration of potassium ions increase, the fluorescence of the CP increases as well (Figure 2). Other cations were similarly analyzed, though sodium, lithium, and ammonium ions did not result in inducing a G-quadruplex, and therefore had weak FRET (Figure 3). The FRET ratio was nearly 16 times higher for potassium ions than that of various cations. Different polymers have also been developed to detect lithium and sodium ions, as well as  $Eu^{3+}$ ,  $Cu^{2+}$ ,  $Co^{2+}$ , and  $Fe^{3+}$ .<sup>2</sup> The last three were detectable through the

use of a poly(p-phenylene)<sup>2</sup>. The presence of these cations shifts the absorption and fluorescence spectra of the specifically designed CP in order to allow for quantitative measurements of the analyte<sup>3</sup>.

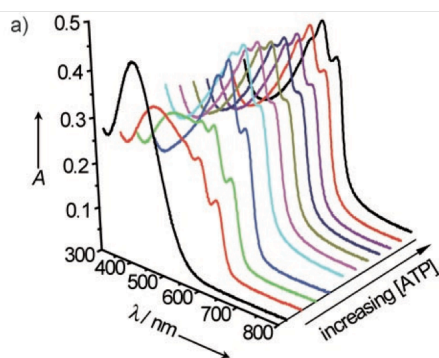
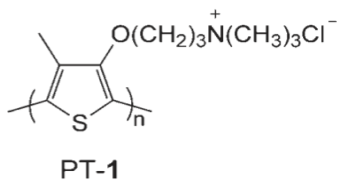


Figure 4. The CP, PT-1, used to detect ATP is shown. In the presence of increasing ATP, front to back, demonstrates a 138nm red shift in the CP's absorption.

In the early 1990s, conjugated polymers became highly involved in biosensing due to its amplification process<sup>2</sup>. An achiral cationic poly(thiophene) CP was also developed to detect ATP in water (Figure 4)<sup>4</sup>. With increasing ATP or ADP concentrations, the initially random-coiled achiral conformation of the CP shifted to a chiral  $\pi$ -stacked aggregated complex. The maximum absorption of the random coils occurs at 400nm with a yellow color, though when the aggregated CP is formed, the maximum absorption shifts to 538nm with a purple colored solution (Figure 4). The paper attributes this to the more planar conformation in the CP that is formed and the strong intermolecular  $\pi$ -stacking interactions. ADP and AMP were similarly analyzed, though these nucleotides did not induce a chiral complex. This implied that indeed the aggregation was a result of the amount of negative charge present. They suggested

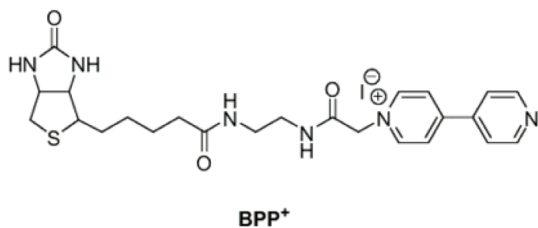
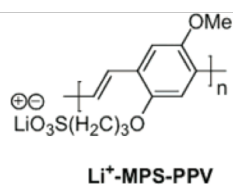


Figure 5. The structures of BPP<sup>+</sup>, the quencher, and the CP, Li<sup>+</sup>-MPS-PPV, are shown.

that this was due to the multiple electrostatic interactions between the triphosphate and the ammonium groups on the CP that causes the more-ordered conformational change.

Many of these assays involve the direct interaction of the analyte. The target affects the moieties near or on the CP to shift absorbance of fluorescence spectra in order to create an optimal signal<sup>2</sup>. For instance, an anionic water soluble CP was used to detect avidin using a biotin-modified fluorescence quencher<sup>1</sup>. When the quencher BPP<sup>+</sup>, bound to biotin, is added to a solution of Li<sup>+</sup>-MPS-PPV, an electrostatic complex is formed between the CP as

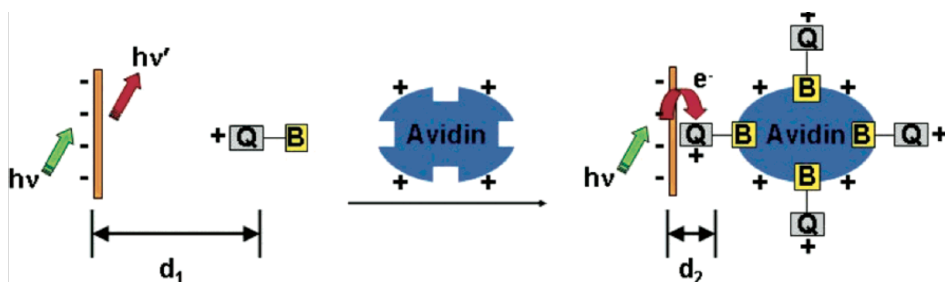


Figure 6. The positively charged avidin selectively binds with the biotin-quencher, which promotes association with the CP.

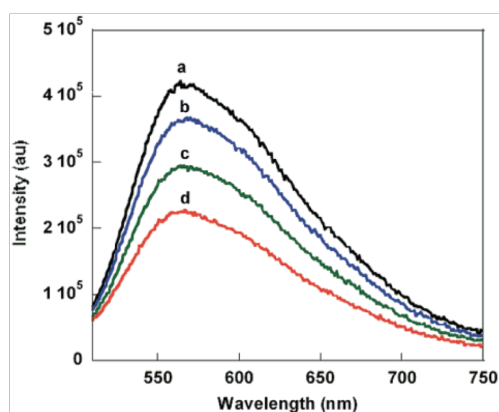


Figure 7. Fluorescence spectra of  $\text{Li}^+$ -MPS-PPV when  $\text{BPP}^+$  is present in a  $0.1\text{M}$   $(\text{NH}_4)_2\text{CO}_3$  at pH 8.9. Avidin concentrations are increased in each solution from a to d.

well as the  $\text{BPP}^+$  quencher (Figure 5). In previous experiments, when avidin is added to the solution, it was thought that the selective binding between avidin and biotin draws the quencher away from the CP. Essentially,

the distance between the CP and the quencher is increased once avidin forms a conjugate with biotin, restoring the fluorescence of CP in a non-buffered solution. This paper proposed a new pathway in with  $\text{BPP}^+$  binding to positively charged avidin enhances the electrostatic attractions to the negatively charged CP (Figure 6). This draws the quencher in for closer association, allowing for a more enhanced quenching effect. The use of a buffered system leads to diminished non-specific interactions and enhances electrostatic attractions between the  $\text{BPP}^+$  and the CP; this increases the quenching effect rather than what was previous

thought to decrease quenching as the concentration of avidin was increased (Figure 7). It is evident that nonspecific interactions, due to electrostatic attraction, may detrimentally affect biosensing with CPs. This paper indicated that the fluorescence was not restored due to specific biotin-avidin interactions, as previously assumed, or steric hindrance, but rather nonspecific interactions between the cationic protein and the anionic polymer. In the presence of aqueous buffer, however, the results are opposite. Hydrophobic interactions between the biotinylated quencher and the polymer became important. Avidin addition did not increase polymer's fluorescence as it did in water. Instead, the fluorescence was better quenched. It was suggested that this was due to avidin-quencher conjugate that was able to form. The positively charged avidin, and the quencher, was less affected by electrostatic interactions due to the buffered solution and was able to better associate with the anionic polymer.

Detection of DNA using FRET and cationic CPs was also developed<sup>5</sup>. Because FRET involves energy transfer from an excitable donor to an acceptor, CPs can potentially be incorporated into this well developed analytical technique as the donor. These CPs have the ability to make FRET more efficient since excitons can migrate to a point in which energy transfer is more efficient. This would amplify the fluorescence and increase sensitivity due to a signal: noise increase. An example of this detection is the following: an acceptor labeled probe

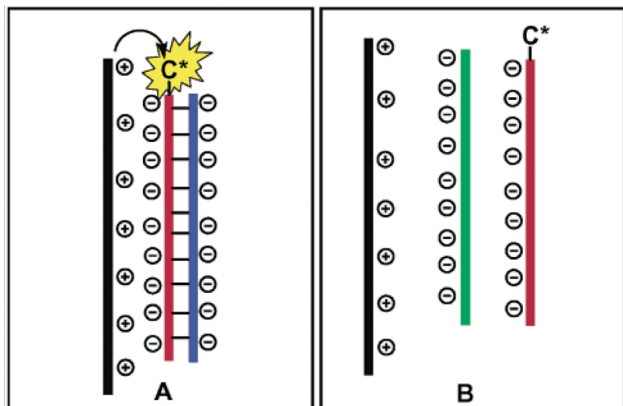


Figure 8. A demonstrates that hybridization between the probe and the target ssDNA strongly associates with the CP, unlike the nonhybridized strand as seen in B.

peptide nucleic acid and a cationic donor, poly(fluorene-co-phenylene). This system has the ability to detect the analyte, DNA with a specific base sequence. Essentially, a fluorophore labeled-ssDNA (Figure 8, in red) can associate with the target complementary strand (in blue) and promote electrostatic interactions with the CP (in black) due to a stronger local charge density of the dsDNA. In the case of a noncomplementary strand (in green), the nonhybridized strand interferes with the association between the

fluorophore labeled-DNA and the CP, resulting in low FRET. In a second detection scheme, the fluorophore labeled probe base pairs with the ssDNA molecule, even though the probe contains neutral amide linkages rather than phosphate linkages. This replacement reduced any probe-CP interaction. When appropriate base pairing has occurred, the probe-DNA complex has a strong negative charge due to the phosphate backbone of the hybridized strand, causing it to associate with the cationic CP. The distance between the donor, the CP, and the acceptor, the probe, has been reduced to Forster distances to allow for efficient FRET to occur. This method eliminates the use of multiple probes while increasing the signal. Electrostatic attracts can be used to control average distance between the CP and the fluorophore in FRET. CPs can be optimized in order to become practical detection methods.

Singlet oxygen ( $^1\text{O}_2$ ) is the lowest excited electronic state of molecular oxygen<sup>3</sup>. As a strong oxidizing agent, it can be biologically toxic to biomolecules including DNA, RNA, and proteins<sup>6</sup>. Singlet oxygen is produced by electron-exchange energy transfer from a photosensitizer, such as Rose Bengal or Eosin-5-isothiocyanate, to triplet oxygen. It has been

shown that singlet oxygen generation can be used as a noninvasive form of photodynamic therapy for destroying cancer cells<sup>3</sup>. Current optical probes for singlet oxygen include 9,10-diphenylanthracene and 9,10-dimethylantracene<sup>6</sup>. These rely on binding specifically to singlet oxygen to form thermodynamically stable endoperoxides. Singlet oxygen is a form of highly reactive oxygen species that specifically reacts and converts polyaromatic acenes into endoperoxides through a Diels Alder mechanism<sup>7</sup>. As the number of rings in the polycyclic

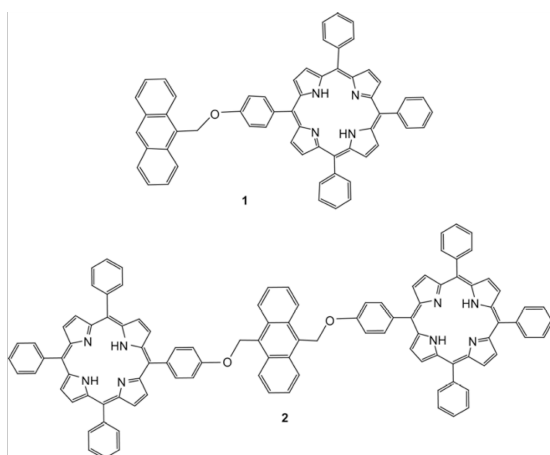


Figure 9. The anthracene derivatives used to detect singlet oxygen.

aromatic hydrocarbons increase, their reactivity does so as well. The central ring is the most reactive, and reacts with singlet oxygen in either a stepwise or a concerted [4+2] cycloaddition mechanism<sup>4</sup>. These anthracene derivatives are further being studied in order to improve selectivity and sensitivity (Figure 9)<sup>6</sup>.

Advancements also include developing metal complex, such as europium (III) and rhenium (I) complexes, as fluorescent probes for singlet oxygen. Conjugated polymers use excited states to help detect levels of singlet oxygen. This

chemical signal avoids any small distance barrier and any non-specific interactions between the fluorophore and the quencher. Previous examples of this method include Nagano's fluorophores bound to an anthracene<sup>8</sup>. After reaction with singlet oxygen, an endoperoxide formed and increased the fluorescent intensity. Despite some successful fluorescent methods, it is necessary to improve the reliability of quantitative measurements in order to allow fluorescent conjugated polymers to be applicable on a large scale.

A comparison of enzyme-linked immunosorbent assay (ELISA) and luminescent oxygen channeling immunoassay (LOCI) was conducted in order to quantify Insulin Aspart (IAsp) in human serum<sup>9</sup>. Because IAsp is an insulin homologue to treat diabetes, large sample sizes are produced during its development. LOCI is a bead based assay that eliminates washing steps and reduces the incubation time from 20-24 hrs for ELISA to 1.5 hrs with LOCI. Additionally, LOCI uses 384-well plates whereas ELISA is optimized for 96-well plates which allows for less throughput. LOCI involved sample incubation with donor biotinylated specific antibody for

Insulin Aspart and insulin-detecting antibody coated acceptor beads. After an hour, streptavidin coated acceptor beads were added to the solution for 30 min. In the presence of IAsp, the two beads are brought in close proximity and a chemiluminescent reaction on the beads occurred, allowing for the detection of light. It was demonstrated that LOCI also has greater sensitivity, precision, as well as a wide range compared to ELISA analysis for detecting biomolecules. ELISA requires washing steps in order to separate bound and free ligand, which increases the workload significantly with large samples<sup>10</sup>. Other methods such as LOCI avoid this since the signal arises from specific molecular binding events. Enzyme channeling immunoassays involves two enzymes binding. One produces a chromogenic substrate for the second enzyme. LOCI overcomes the extra procedural steps in ELISA by nonenzymatic use of singlet oxygen to allow for real time monitoring of particle interactions. Here, singlet oxygen diffuses to a substrate to induce a chemiluminescent reaction at the reaction site.

The development of these types of assays involves overcoming previous limitations and drawbacks found in ELISA. ELISA has a high limit of detection, greater than the pM range. In addition, ELISA results in false positives and negatives as a result of enzyme use, resulting from insufficient antigen coating. This project employs the use of a ratiometric signal, allowing more certainty in the quantitative conclusions of these assays. Using conjugated polymers together with singlet oxygen photosensitization is demonstrated to significantly increase the chemical signal's amplification. Intensity changes themselves can be unhelpful since fluorophore concentration in each location of the cell cannot be controlled and the continuously changing fluorophore concentrations<sup>11</sup>. Therefore, wavelength ratiometric probes were used in order to allow for these measurements to be independent of fluorophore concentration. The development of these singlet oxygen sensitive conjugated polymers has the potential to develop and improve chemical and biological analytical methods. Such applications include the non-enzymatic signal amplification with high sensitivity as well as improved accuracy and quantification of assays through the use of wavelength ratiometric responses.

Essentially, a platform of thin films, containing an acene doped conjugated polymer host, demonstrates a ratiometric fluorescence response to singlet oxygen was created. An initial platform using Singlet Oxygen Sensor Green (**SOSG**) as a singlet oxygen detector was also created and compared to the more enhanced acene/conjugated polymer film. These thin films were designed to display a ratiometric fluorescent response to singlet oxygen specifically in an

aqueous environment. The development of these films transitioned into creating a biochemical binding event in an aqueous solution. The second objective of this project is to use these conjugated polymers to detect singlet oxygen with a low limit of detection and high selectivity. These conjugated polymers amplify quenching since the excited states can move along the CP's backbone in a process so that one quencher has the ability to quench all the excited state. Essentially, the 5, 12-bis(4-methoxyphenyl)tetracene (**TET**) quenches the fluorescence from the conjugated polymer backbone. This is especially amplified in solid state since even in low concentrations of the fluorescent trap, the conjugated polymer efficiently donates energy or results in photoinduced electron transfer. The use of solid state films throughout these experiments requires less acene concentration for the same amount of energy transfer to occur. This is mainly due to excited states in solid states are more efficient than compared to in solutions. To avoid problems with ionic CPs for biosensing, nonionic and water soluble CPs can be synthesized by incorporating hydrophilic groups<sup>2</sup>. A hydrophobic thin film then provides favorable interactions for the quenchers. Therefore, biosensing with hydrophobic CP containing thin films are less likely to have nonspecific interactions than their counterpart. The buffered solutions allow for less interference from electrostatic changes compared to systems using polyelectrolytes<sup>2</sup>.

The project combines both a chemical amplification as well as an optical amplification through the binding of singlet oxygen. The photosensitizer of singlet oxygen is bound to the secondary analyte. When stimulated with light, the solution containing oxygen and the bound photosensitizer yields singlet oxygen. This chemical amplification of singlet oxygen then reacts with conjugated polymer traps. When singlet oxygen binds to polycyclic aromatics, the conjugated polymers are quenched and destroyed. Individual traps on the conjugated polymer film which react with singlet oxygen then emit photons, producing an optical amplification. Therefore, acene substituted conjugated polymers will have an increased fluorescence signal after exposure to singlet oxygen. Initially, only the quencher's fluorescence is emitted due to energy transfer from the conjugated polymer to the **TET** pendants. There is an overlap between the polymer's absorption and **TET**'s emission which allows for the excited state to be transferred. When singlet oxygen is introduced through the photosensitizer, the fluorescence shifts from the **TET** to the conjugated polymer backbone at 420 nm as endoperoxides on the **TET** are formed. When the photosensitizer is bound to NeutrAvidin-biotinylated microspheres,

singlet oxygen is still generated; the singlet oxygen then reacts with the TET on the thin films to restore the CP's fluorescence (Figure 10).

This proposed method allows for several improvements in the current analytical methods available. Using a photosensitizer bound to a secondary analyte rather than an enzyme avoids any detrimental interferences enzymes present. An enzyme can decrease selectivity by exacerbating non-specific binding of secondary analytes or due to the instability of enzymes. Secondary, the use of a wavelength ratiometric response allows for improved quantification and reduces the amount of false positives and negatives. It also provides better control since reactions are light activated. Singlet oxygen provides a longer range of up to 200nm in water for distance dependent reactions.

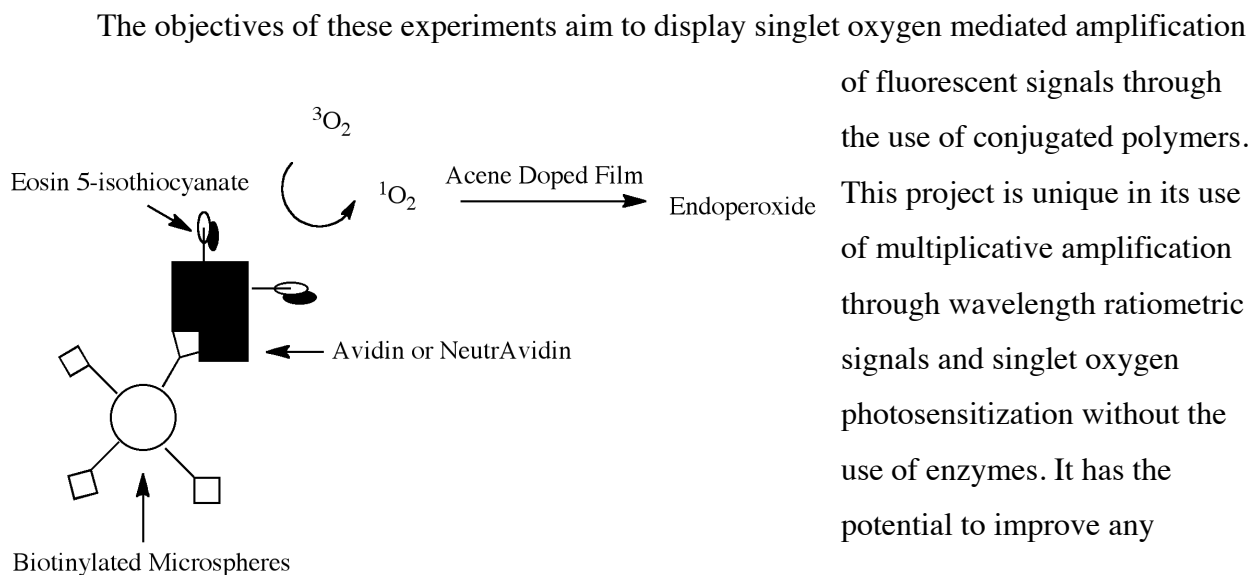


Figure 10. Schematic of **BNE** experiments is shown. The eosin 5-isothiocyanate, bound to NeutrAvidin/Biotinylated Microspheres (**BNE**), are irradiated to produce singlet oxygen. Singlet oxygen then reacts with **TET** on the thin films to yield non quenching endoperoxides.

involve the use of sandwich fluorescent assays such as analysis of clinical samples. This combination of advantages of this developing method allows for the creation of new analytical methods that allow for highly improved fluorescent signal amplification in a variety of applications.

## Experimental

### Conjugated Acene Characterization

#### Kinetic Experiments of Conjugated Acenes with $^1\text{O}_2$

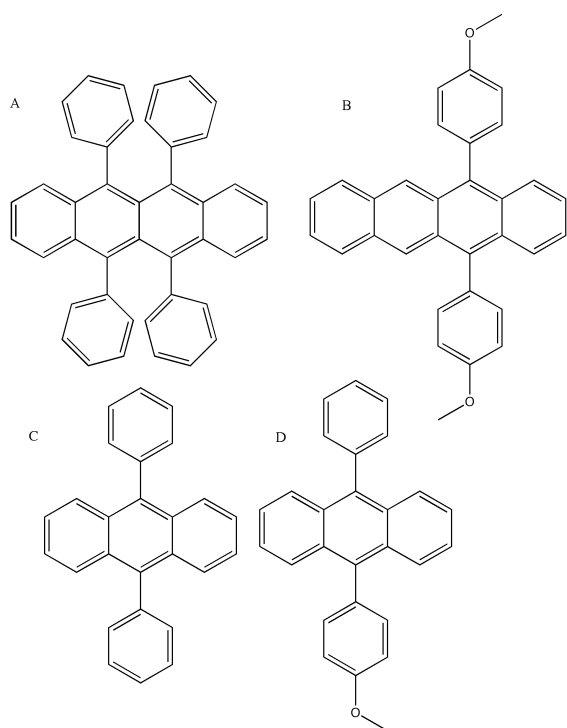


Figure 11. Structures of A) rubrene, B) TET C) 9, 10 diphenylanthracene, and D) MANT are shown.

All absorbance spectra were collected with a Varian Cary-100 UV-Vis spectrophotometer in the double beam mode with solvent containing cuvette for background subtraction spectra. To generate singlet oxygen, methylene blue photosensitizer was irradiated with a 200W Hg/Xe lamp (Newport-Oriel) equipped with a focusing lens and a 590nm long pass filter. A stock solution of methylene blue was prepared to have an absorption of 1.0OD at its maximum peak. 5, 12-bis(4-methoxyphenyl)tetracene (**TET**) was then dissolved at a concentration of 0.01M in  $\text{CDCl}_3$ . This solution was diluted 100 fold with the previously prepared methylene blue stock solution to yield a final

**TET** concentration of 0.1mM. An initial absorbance approximately 1.0 for the characteristic tetracene peaks was recorded. The solution containing cuvette was

placed 30 cm in the focal point of the light source, using a 590nm long pass filter and convex lens. The solution was then irradiated at time intervals prior to the acquisition of each absorbance spectrum. This was continued until the sample's absorbance was approximately 0.01OD. This procedure was repeated several times for **TET**, 9-(4-methoxyphenyl)-10-phenylanthracene (**MANT**), and 9, 10 diphenylanthracene in both  $\text{CDCl}_3$  and DCM (Figure 11). The wavelengths for kinetic analysis for **TET** was 496nm; 9-(4-methoxyphenyl)-10-phenylanthracene was 376nm; and 9, 10 diphenylanthracene was 375nm. Methylene blue photosensitizer would not dissolve in diethyl ether or benzene, whereas the tetracene molecule would not dissolve well in acetone. Therefore, reaction rates in DCM and  $\text{CDCl}_3$  were conducted.

### **5, 12-bis(4-methoxyphenyl)tetracene Quantum Yield & Extinction Coefficient**

A stock solution of **TET** of concentration  $46\mu\text{M}$  was prepared in DCM. Serial dilution was used to obtain  $23\mu\text{M}$ ,  $6.9\mu\text{M}$ , and  $1.4\mu\text{M}$  of the **TET** molecule in DCM. Absorbance spectra of each concentration were recorded. Analysis of the absorbances at 495nm corresponding to the **TET** molecule was performed. This method was repeated once more to obtain an average extinction coefficient.

A stock solution of Coumorin 6 in ethanol was prepared. A background spectrum of ethanol was also used while preparing a solution of Coumorin 6 with an absorbance less than 0.10OD from the Coumorin 6 stock solution. A stock solution of **TET** prepared in DCM. This solution was diluted until the absorbance was  $<0.10\text{OD}$  while subtracting DCM background signal. The absorbances of both Coumorin 6 and tetracene at 435nm were recorded for quantum yield calculations. Fluorescence emission spectra were taken by using a PTI Quantum Master 4 equipped with a 75 W Xe lamp. The solution containing cuvettes were then analyzed using the fluorimeter at excitation wavelength 435nm, emission wavelength 445-750nm, excitation and emission slit widths of 2nm, integration of 0.5sec. This method was repeated once more to obtain an average quantum yield of **TET**.

### **5, 12-bis(4-methoxyphenyl)tetracene Endoperoxide Formation & Separation**

38mg of the **TET** molecule was dissolved in  $\text{CDCl}_3$ , containing a small amount of methylene blue photosensitizer. The solution was irradiated with a 590nm filter and a focusing lens while bubbling oxygen through for 30 min. An  $^1\text{H}$  NMR was taken to confirm endoperoxide formation. Silica gel column chromatography was performed using 7 DCM: 3 hexanes (v:v) to separate two endoperoxides. Thin layer chromatography was also performed with 7 DCM: 3 hexanes (v:v) for both endoperoxides. The first endoperoxide eluted had an  $R_f$  value of 0.69, while the second had an  $R_f$  value of 0.57.  $^1\text{H}$  NMR scans of the two endoperoxides were taken.

### **Avidin-Eosin 5-isothiocyanate Conjugate Experiments with $^1\text{O}_2$ using SOSG**

#### **Labeling and Gel Filtration**

10 mg of avidin was dissolved in 1 mL of 0.1 M pH 9 sodium bicarbonate buffer. The buffer solution was made by dissolving 2.386 g sodium bicarbonate and .1694 g sodium carbonate in 200 mL Millipore water. In a second vial, 5 mg of eosin-5-isothiocyanate (Invitrogen) was dissolved in .5 mL of DMF immediately before it was added to the avidin

solution. 100  $\mu\text{L}$  of the eosin 5-isothiocyanate solution was added to the protein solution, with continuous stirring for an hour at room temperature. The solution was stored in the refrigerator. In order to separate the avidin-eosin 5-isothiocyanate conjugate (**AE**) from excessive dye, a Sephadex column was prepared. Approximately 5 g of Sigma Sephadex G-50 was allowed to swell overnight in excess distilled water. The column was prepared using 0.1 M pH 9 sodium bicarbonate buffer as the eluent. The first red band collected contained a broad peak at 525 nm

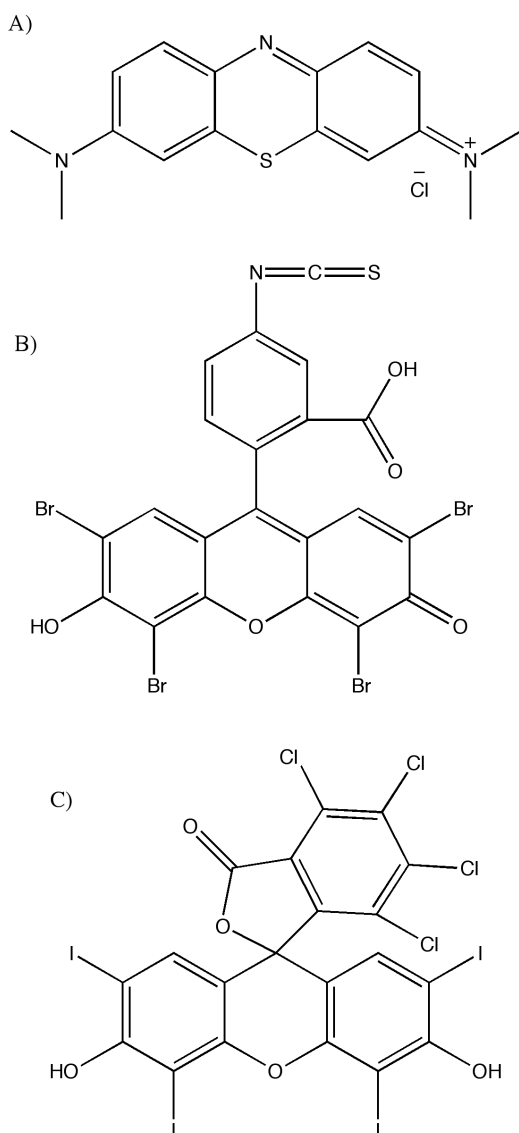


Figure 12. Three singlet oxygen photosensitizers, A) Methylene Blue B) Eosin 5-isothiocyanate C) Rose Bengal, are shown.

and a second notable absorbance at 280 nm, corresponding to eosin and avidin-eosin respectively. The second light red sample collected displayed a small peak at 525 nm, but did not contain a peak at 280 nm. Since eosin absorbs light at its peak near 525nm and avidin contains tyrosine and tryptophan, which absorb at 280nm. Hence, the sample containing these two characteristic peaks at 525nm and 280nm is indicative of the **AE** conjugate. The solution containing **AE** was used for the following experiments. The degree of labeling was 5.43 (Appendix Eq 1).

### Experiment: Avidin-Eosin 5-isothiocyanate & SOSG Spectrophotometry

An initial 100% transmittance scan was taken with both cuvettes containing 0.1 M pH 9 sodium bicarbonate buffer using a Varian Cary-100 UV/Visible Spectrophotometer in double beam mode. The experimental cuvette was replaced with a solution of **SOSG** (Invitrogen) and **AE** to obtain an absorbance of approximately 0.6 at 525nm or until the signature peaks were seen. The **SOSG** stock solution was created by dissolving **SOSG** in 0.1 M pH 9 sodium bicarbonate buffer. After an initial absorbance scan, the sample was placed 20 cm from an ozone-free 200W Hg/Xe Newport-Oriel

lamp using a 515 nm filter. Simultaneously, oxygen was bubbled through the cuvette for 10 min. A second absorbance scan was taken, after which the sample was irradiated and bubbled through with oxygen for 10 to 15 more minutes. This was repeated until several absorbance scans were taken. Before each scan, the spectrophotometer was zeroed.

#### **Negative Control: SOSG Spectrophotometry**

A similar procedure to the 'Avidin-Eosin 5-isothiocyanate & **SOSG** Spectrophotometry' was followed. However, no **AE** conjugate was added. Before each scan, the spectrophotometer was zeroed.

#### **Negative Control: SOSG Fluorescence**

A 100 % transmittance scan was taken initially of two cuvettes containing the 0.1 M pH 9 sodium bicarbonate buffer. Using the UV-Vis, a solution of **SOSG** with an absorbance of less than 0.1 OD was obtained. An initial fluorescence emission scan was taken as well using the following parameters: Excitation Wavelength 480nm, Emission Wavelength Scan 490-750nm, Slit Width 2 nm, Integration 0.5 s. The sample was placed in front of the lamp, using a 515 nm long-pass filter, while oxygen was bubbled through the solution for 10 min. A second emission scan was taken. This exposure to light and oxygen was repeated twice more.

#### **Positive Control: Rose Bengal & SOSG Fluorescence**

A 100% transmittance scan was taken of two cuvettes containing D<sub>2</sub>O. A stock solution of Rose Bengal (**RB**) in D<sub>2</sub>O was created, as well as a stock solution of **SOSG** in D<sub>2</sub>O. Using the stock solutions, a sample with an absorbance less than 0.1 OD was obtained. The **SOSG** peak was around 507 nm while the peak for **RB** was approximately 547 nm. An initial fluorescence was obtained using the following conditions: Excitation Wavelength 480nm, Emission Wavelength Scan 490-750nm, Slit Width 4 nm, Integration 0.5 s. After 10 min of bubbling oxygen through the solution and exposing it to light, with a 515 nm long-pass filter, a second emission scan was obtained. This was repeated one more time for 15 min rather than 10 min and a third emission scan was acquired.

#### **Positive Control: Eosin 5-isothiocyanate & SOSG Fluorescence**

An initial 100% transmittance scan was obtained using D<sub>2</sub>O in each cuvette. A stock solution of eosin 5-isothiocyanate in D<sub>2</sub>O was prepared. Eosin 5-isothiocyanate and **SOSG** were added to the experimental cuvette until the absorbance was less than 0.1 OD. An initial fluorescence scan was taken with the following parameters: Excitation Wavelength 480nm,

Emission Wavelength Scan 490-750nm, Slit Width 4 nm, Integration 0.5 s. The sample was then placed 20cm from the lamp using a 515 nm filter while bubbling oxygen through for 10 min.

This was repeated three more times for 25 min.

### **Experiment: Avidin-Eosin 5-isothiocyanate & SOSG Fluorescence**

An initial 100 % transmittance scan was taken of two D<sub>2</sub>O solutions. Using the UV-Vis, a solution of **AE** conjugate and **SOSG** with an absorbance of less than 0.1 OD was obtained. An initial fluorescent emission scan was taken using the following parameters: Excitation Wavelength 480nm, Emission Wavelength Scan 490-700nm, Slit Width 4 nm, Integration 0.5 s. The sample was placed in front of the lamp, using a 515 nm filter, while oxygen was bubbled through the solution for 10 min. A second emission scan was taken. This exposure to light and oxygen was repeated twice more for 15 min each.

### **Biotin-Avidin-Eosin 5-isothiocyanate Experiments with <sup>1</sup>O<sub>2</sub> using SOSG**

#### **Avidin-Eosin Attachment to Biotin**

To prepare a 0.1M pH 7.4 PBS solution, 0.650 g NaH<sub>2</sub>PO<sub>4</sub>, 5.425g Na<sub>2</sub>HPO<sub>4</sub>-7H<sub>2</sub>O, and 2.1925 g NaCl was dissolved in 250 mL Millipore water. 1 mL of Biotin Coated Microspheres (Bangs Laboratories, Inc) was washed with 10 mL of PBS and centrifuged three times, each time discarding the supernatant. The final pellet of biotinylated microspheres was resuspended to a final concentration of 0.5 mg/mL using 20 mL PBS. The original biotinylated microsphere concentration was 10 mg/mL, so the pellet was diluted to 20 mL solution. The **AE** conjugate was added to the suspension of microspheres while stirring gently for 30 min at room temperature. The final product was washed three times with PBS. The microspheres bound to **AE** were stored in a PBS solution.

#### **Experiment: Biotin-Avidin-Eosin & SOSG Spectrophotometry**

An initial 100% transmittance was recorded for two cuvettes containing D<sub>2</sub>O. **SOSG** and the biotinylated microspheres with eosin-tagged protein was added to the experimental cuvette until the solution had an absorbance of approximately 0.17 or when the characteristic peaks 300 to 400 nm can be seen. The solution was then placed in front of the lamp, with a 515 nm filter, while bubbling oxygen through for 10 min. Absorbance was then measured. This was repeated four more times.

**Experiment: Biotin-Avidin-Eosin & SOSG Fluorescence**

A 100% transmittance scan was taken of two solutions of D<sub>2</sub>O. **SOSG** and the biotinylated microspheres-avidin-eosin 5-isothiocyanate (**BAE**) complex were added to the solution, adjusting the absorbance to under 0.1 OD. The fluorescence of this solution was measured using the following conditions: Excitation Wavelength 480nm, Emission Wavelength Scan 490-700nm, Slit Width 4 nm, Integration 0.5 s. The solution was placed in front of the lamp using a 515 nm long-pass filter while bubbling oxygen through for 10 min. A second fluorescent scan was then taken. This was repeated three additional times.

**Negative Control: Washed Biotinylated Microspheres, Eosin 5-isothiocyanate, & SOSG Fluorescence**

A 100% transmittance scan was taken of two samples of D<sub>2</sub>O. **SOSG** and washed biotinylated microspheres, without the bound avidin-eosin 5-isothiocyanate conjugate, and amine reactive eosin 5-isothiocyanate was added to the solution. The washed biotinylated microspheres were prepared using 0.5 mL of 10mg/mL biotin and resuspending them in 5mL 0.1 M pH 7.4 PBS. The solution was centrifuged after which the supernatant was removed. This was done twice more, resuspending the final biotin in the PBS solution. The absorbance was adjusted until it was less than 0.1 OD. The fluorescence of this initial solution was measured using the following conditions Excitation Wavelength 480nm, Emission Wavelength Scan 490-700nm, Slit Width 4 nm, Integration 0.5 s. The solution was placed in front of the lamp, using a 515 nm filter, while oxygen was bubbled through the solution for 10 min. A second emission scan was taken; this exposure to light and oxygen was repeated twice more for 15 min each.

**Negative Control: Washed Biotinylated Microspheres & SOSG Fluorescence**

After a 100% transmittance scan of two D<sub>2</sub>O solutions, washed biotinylated microspheres and **SOSG** was added to the experimental sample until the absorbance was less than 0.1 OD. An initial fluorescence emission scan was taken using the following parameters: Excitation Wavelength 480nm, Emission Wavelength Scan 490-700nm, Slit Width 4 nm, Integration 0.5 s. The sample was placed in front of the lamp, using a 515 nm filter, as oxygen was simultaneously bubbled through the solution for 10 min. Three more spectra were taken in a similar fashion.

## Tetracene/Poly(fluorene) Film with Rose Bengal Experiments

### Spun-cast Film Preparation

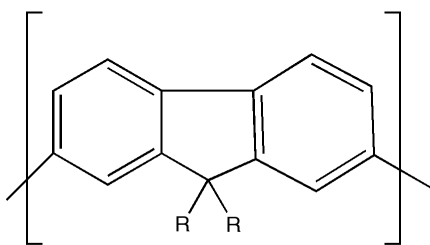


Figure 13. Poly (9, 9-di-n-dodecylfluorenyl-2, 7-diyl)'s (PF) structure is shown.

A solution containing 10% **TET** to poly (9, 9-di-n-dodecylfluorenyl-2, 7-diyl) (**PF**) was prepared by dissolving 5 mg of **TET** and 50 mg of **PF** in 5 mL  $\text{CHCl}_3$ . After sonication, the solution was filtered using a VWR .45  $\mu\text{m}$  PTFE 13mm syringe filter. This solution was spun-cast onto a Fisher Scientific 22X22 mm microscope cover glass film using a Laurell Technologies Corporation spin coater (Model WS-400 BZ-6NPP/Lite). The program for the spin-coater was spinning at 500 rpm for 3 s (acceleration of 330 rpm/s)

followed by spinning at 1500 rpm for 20 s (acceleration of 1650 rpm/s).

### Fluorescent Spectroscopy Parameters

The excitation wavelength was set to 365 nm corresponding to the emission scan from 400 to 600 nm. The step size was set to 5 nm and the integration to 0.1 sec. A quick emission scan of the **TET:PF** film was established to avoid any reaction with the oxygen and light. A slit width of 2 nm allowed an appropriate light intensity. Each experiment used a fresh, unreacted **TET:PF** film in a new solution of **RB**.

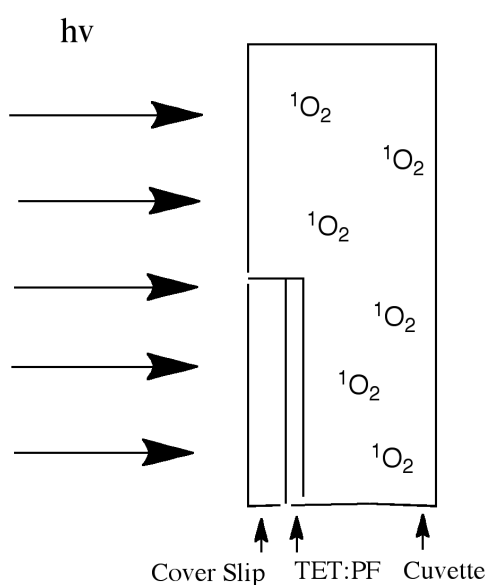


Figure 14. The set up of all **TET:PF** film experiments. The cuvette contains either a control solution or a photosensitizer containing solution that produces singlet oxygen, which can react with the **TET**.

### Initial Negative Controls

As an initial negative control experiment, the 10% dimethoxyphenol tetracene/poly (9, 9-di-n-dodecylfluorenyl-2, 7-diyl) film was irradiated using a 515 nm long pass filter (Figure 13). After a period of exposure, the film's fluorescence spectrum was observed. Similarly, the film was rotated with no additional light exposure in order to obtain another emission spectrum. This was repeated several times to obtain different **TET** spectra with varying fluorescence intensities. As a second negative control, the film was placed in distilled water for 1 min before being irradiated with light using the 515 nm filter.

This placement in water and exposure to light was repeated

several times. The final negative control experiment involved placing the film in a solution of Rose Bengal and distilled water for continuous 1 min intervals with no exposure to light.

### **10% TET:PF Film with a 515 Band Pass Filter with Varying RB Concentrations**

The film was placed in a solution of Rose Bengal and distilled water for 1 min before irradiating it for 5 minute (Figure 14). The emission spectrum was then observed. This exposure to Rose Bengal in distilled water for 1 min and drying the film before irradiation placement for 5 min intervals was repeated four more times. This experiment was replicated a second time. A stock solution of 1mM Rose Bengal was prepared by dissolving 0.0153 g **RB** in 15 mL of distilled water. An initial emission spectrum of a 10% **TET:PF** film was taken. The film was then placed in a quartz cuvette 4cmX1cmX1cm so that the side containing the spun-cast **TET:PF** was exposed and completely submerged in the **RB** solution. The side of the film with no reactants was pressed against the cuvette. This side was oriented in order to be exposed to the light with a 515 nm filter. This film was then irradiated while being in the Rose Bengal solution for 5 min. The film was removed from the solution, rinsed with distilled water, and gently patted dry with a Kimwipe. A second emission spectrum was taken of the film. This experiment was repeated, exposing a new **TET:PF** film to light and a fresh solution of **RB** for 6 min and 12 more min taking spectra after each exposure. This experimental set up with an unreacted **TET:PF** film was repeated after replacing the 1mM Rose Bengal solution with 1 $\mu$ M Rose Bengal solution. This was prepared by diluting 15  $\mu$ L in 15 mL of distilled water. The film's exposure time to both the light and Rose Bengal was 6 min intervals for 18 min. This experiment was replicated replacing the 1 $\mu$ M Rose Bengal solution with a 1nM Rose Bengal solution. Between each emission spectrum measurement, the film was exposed to light and the Rose Bengal solution for 5 min intervals for 15 min.

### **10% TET: PF Film with Varying Filters**

In the next experiments the filter used for the lamp was varied. In a control experiment, the film was placed in the cuvette containing distilled water with no singlet oxygen photosensitizer. The 515 nm long pass filter was used. As before, an initial emission spectrum was taken of the film. The film was then placed in the cuvette in a similar method as previously mentioned while irradiating for 5 min intervals for 25 min. A second experiment was performed using a 515 nm long pass filter with a 1  $\mu$ M Rose Bengal solution for 5 min intervals for 20 min. A third experiment was performed with a 1x10<sup>-5</sup> M Rose Bengal solution for 5 min intervals for

20 min. These three experiments were repeated replacing the filter from 515 nm long pass filter to a 546.1 nm interference filter and a 570 nm long pass filter.

Using a 546.1 nm interference filter, the 10% **TET:PF** film was placed in the cuvette containing 1  $\mu$ M Rose Bengal solution in D<sub>2</sub>O. After each interval of 5 min for up to 20 min, an emission spectrum was taken. This experiment was repeated four more times with intervals of approximately 5 min.

### **Varying Percentages TET:PF Films with a 546.1 nm Filter in 1 $\mu$ M RB/ D<sub>2</sub>O**

Experiments previously described were performed using a 546.1 nm filter with varying **TET** amounts. A stock solution of 10% **TET** solution was prepared by dissolving 0.005 g of tetracene in 5 mL CHCl<sub>3</sub>. 2.5mL of this 10% **TET** stock solution was diluted to 5 mL to prepare a 5% **TET** stock solution. To prepare a 2.5% **TET** stock solution, 2.5 mL of the 5% solution was diluted to 5 mL. 2 mL of the 2.5% **TET** was then diluted to 5 mL to create a 1% stock solution. To each solution, .0250g **PF** was added. The 10% **TET:PF** solution contained a final concentration of .0023M **TET** and .0010M **PF**. The final concentrations of **TET** and **PF** in the 5% solution were .0011M and .0010M, respectively. The 2.5% **TET: PF** solution contained .00057M **TET** and .0010M **PF**. Lastly, the 1% solution contained a final concentration of .00023M **TET** and .0010M **PF**. For each experiment, a fresh film was placed in a 1  $\mu$ M Rose Bengal and irradiated as previously mentioned for 5 min intervals for 15-20 min. For more detailed measurements, 1 min intervals were used initially for 10 min and increasing to 10 and 20 min exposures to light and Rose Bengal for the 2.5% film. For the 1% film, 1 min intervals were performed for 5 min, increasing to 3 min, 4 min, 8 min, and 10 min intervals for 30 min. These experiments were repeated 2 more times for each type of **TET:PF** film.

### **2.5% TET: PF Films with a 546.1 nm Filter in Varying RB Concentrations**

In order to find the lowest concentration of Rose Bengal that produces a response on a 2.5% tetracene: poly(fluorene) film, varying concentrations of **RB** were used. A 546.1 nm interference filter was used to irradiate a 2.5% film in 100 nM **RB** in D<sub>2</sub>O for 5 min intervals for 20 min. A 10 nM **RB** solution was then used with 10 min exposure to light and the photosensitizer for 60 min. A 1 nM **RB** solution was used in the following experiment for 10-15 min intervals for 50 min. A negative control experiment was performed placing the film in D<sub>2</sub>O containing no Rose Bengal. This was irradiated for various times for approximately 10 min intervals for up to 2 hours.

### **2.5% TET:PF Film in Biotinylated Microspheres/Avidin/Eosin Solution**

This solution of Rose Bengal was replaced with a solution of biotinylated microspheres bound to an Avidin-Eosin conjugate in 0.1M pH7.4 PBS. A 2.5% film was placed in a cuvette containing **BAE** and irradiated simultaneously with a 515 long pass filter for 10 min intervals for 60 min. A negative control experiment was carried out replacing the **BAE** conjugate with washed biotinylated microspheres in 0.1M pH7.4 PBS.

### **Biotin/NeutrAvidin/Eosin Experiments with TET/PF Films**

#### **2.5% TET:RB Film in Biotin/NeutrAvidin/Eosin Solution**

Biotin-NeutrAvidin-Eosin 5-isothiocyanate (**BNE**) Preparation: 10 mg of NeutrAvidin Biotin Binding Protein (Thermo Scientific) was dissolved in 1 mL of 0.1 M pH 9.0 sodium bicarbonate buffer. 5 mg of eosin-5-isothiocyanate was dissolved in 0.5 mL of DMF immediately before it was added to the NeutrAvidin solution. 100  $\mu$ L of the eosin 5-isothiocyanate solution was added to the protein solution, with continuous stirring for an hour at room temperature. In order to separate the NeutrAvidin-eosin 5-isothiocyanate conjugate from any excessive dye, a Sephadex column was prepared. Approximately 5 g of Sephadex G-50 was allowed to swell overnight in excess distilled water. The Sephadex gel filtration column was prepared using 0.1M pH 9.0 sodium bicarbonate buffer as the eluent. An absorbance spectrum of the band collected thought to contain this conjugate was acquired. The concentration of the protein was determined to be 1.46 $\mu$ M; the degree of labeling of dye to protein was (Appendix Eq 2).

Biotinylated microspheres, 1% solids in 1mL with a diameter of 10  $\mu$ m, were then washed three times with 10mL 0.10 M PBS buffer of pH 7.4. Centrifugation at 4000 rpm for 5 min in between washing steps yielded the microspheres. 10mL of the protein-dye complex was added to the biotinylated microspheres solution. This reaction proceeded for 30 min at room temperature with gentle stirring. The solution was washed and centrifuged three times using 10mL 0.10 pH 7.4 PBS buffer. The NeutrAvidin/Eosin-bound microspheres were stored at 4°C at a NeutrAvidin concentration of 1.46 $\mu$ M.

#### **2.5% TET:PF Films in Varying Concentrations of Biotin/NeutrAvidin/Eosin Solutions**

A stock solution of the **BNE** complex was obtained with a NeutrAvidin concentration 1.46  $\mu$ M. A solution of 1  $\mu$ M **BNE** was prepared through diluting 6.85 mL of the original solution in 10 mL PBS. An initial fluorescence spectrum of 2.5% **TET:PF** film was obtained.

The film was irradiated, using a 515nm long pass filter and focusing lens, after being placed in a 1  $\mu$ M **BNE** solution contained cuvette. In between irradiation exposures, the film was washed with distilled water and dried to obtain a fluorescence spectrum. This was continued until the **TET** emission peaks were unrecognizable. Similar methods were carried out in 100nM, 10nM, and 1nM **BNE** solutions, after dilution from the stock solution of **BNE**. Control solutions were also prepared in the absence of **BNE**, and contained only 0.10M pH7.4 PBS. One control involved binding of 100nM NeutrAvidin to biotinylated microspheres without any eosin 5-isothiocyanate. Also, these methods for 0nM, 1nM, 10nM, 100nM, 1  $\mu$ M **BNE** solutions and 2.5% **TET:PF** films were repeated using a 530 long pass filter. At each concentration of NeutrAvidin, a negative control was performed by placing the film in the **BNE** solution and was not exposed to light throughout the duration of the experiment.

### **2.5% TET:PF Films with Non-biotinylated Microspheres PBS Solutions and 1% Bovine Albumin Serum (BSA) doped PBS Solutions**

100 $\mu$ L of 9.9% solids Polystyrene microspheres with a diameter of 10.11  $\mu$ m were washed and centrifuged three times with either 10mL 0.10 mM PBS of pH7.4 or 0.10mM pH7.4 PBS of containing 1% BSA. The BSA doped PBS solution was prepared by diluting a Blocker BSA (10%) PBS Solution in 0.10 mM PBS. A solution of NeutrAvidin/Eosin 5-isothiocyanate was added to the non-functionalized microspheres for 30 min of gentle stirring at room temperature. The solution was washed and centrifuged as previously mentioned. The final solution was stored at 4°C. An initial emission scan of the 2.5% **TET:PF** film was obtained. The film was placed in a solution of the non-biotinylated microspheres that reacted with the NeutrAvidin/Eosin 5-isothiocyanate conjugate. After the film was placed in the solution, the solution was irradiated with a 530nm filter and focusing lens. In between irradiation times, the film was rinsed with distilled water and dried before emission scans were taken. The methods were repeated replacing the previous PBS solvent with the 1% BSA doped PBS.

## Results & Discussion

### Conjugated Acene Characterization

#### Kinetic Experiments of Conjugated Acenes with $^1\text{O}_2$

When conjugated acenes are exposed to singlet oxygen, endoperoxides were able to form. However, due to steady state approximations, the singlet oxygen concentration does not alter

over time as the acenes do. Instead, the rate of formation of  $^1\text{O}_2$  is equal to that of its consumption. The rate of singlet oxygen formation is a product of the intensity of light  $I_a$ , and the photosensitizer's quantum yield  $\Phi$ . Singlet oxygen has two consumption pathways: 1) reacting with the conjugated acene molecule to yield endoperoxides and 2) reverting back to triplet oxygen. The latter has a first order reaction rate constant of  $1.3 \times 10^4 \text{ s}^{-1}$  for the rate  $=k_d[^1\text{O}_2]$ . The former reaction is

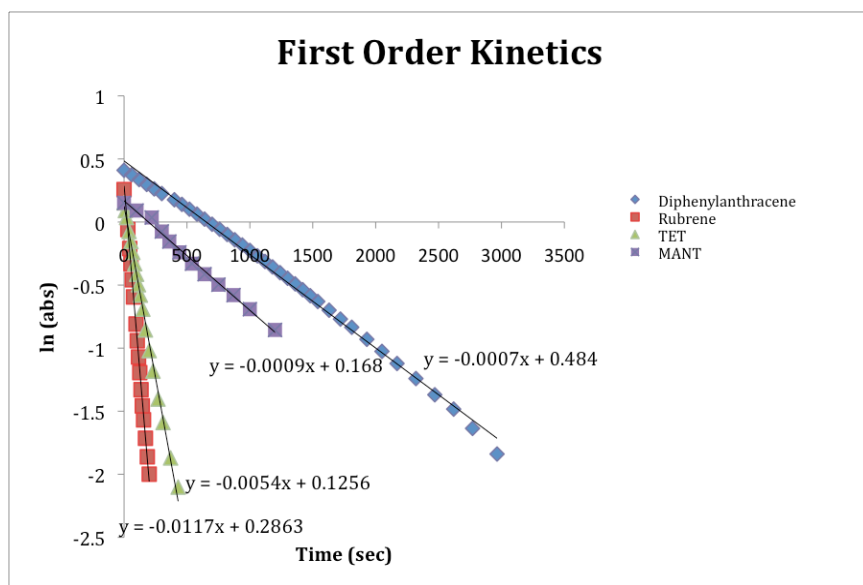


Figure 15. First order kinetics of four conjugated acenes when exposed to singlet oxygen are shown. A linear relationship between  $\ln(\text{Absorbance})$  and the time demonstrate the pseudo first order kinetics due to steady state approximations of

such:  $\text{acene} + ^1\text{O}_2 \rightarrow \text{endoperoxides}$ . The rate of reaction is therefore  $\text{Rate} = k_a[\text{Acene}][^1\text{O}_2]$ , with  $k_a$  as the reaction rate constant multiplied by the acene and singlet oxygen concentrations. This rate constant is  $3 \times 10^6 \text{ M}^{-1} \text{ s}^{-1}$  while the acene concentration is calculated to be around  $10^{-5} \text{ M}$ .

Because the  $k_d$  is much larger than  $k_a[\text{Acene}]$ , this term can be omitted when placing the two destruction pathways equal to the production of  $^1\text{O}_2$ . The equation can be rearranged from  $I_a * \Phi = k_d[^1\text{O}_2] + k_a[\text{Acene}][^1\text{O}_2]$  to  $[^1\text{O}_2] = (I_a * \Phi) / (k_d + k_a[\text{Acene}])$ . The reaction observed is  $\text{acene} + ^1\text{O}_2 \rightarrow \text{endoperoxides}$ , whose rate of reaction is  $-d[\text{endoperoxide}]/dt = k_r[^1\text{O}_2][\text{Acene}]$ , with  $k_r$  as the observed reaction constant. Taking into account the omitted term and substituting the  $[^1\text{O}_2]$  yields  $-d[\text{endoperoxide}]/dt = k_r[(I_a * \Phi) / (k_d)] [\text{Acene}]$ . It is shown that  $[^1\text{O}_2]$  is held in steady state since the term  $[(I_a * \Phi) / (k_d)]$  is constant. This bimolecular reaction is indeed pseudo-first order. In similar conditions of singlet oxygen photogeneration, **TET**, 9, 10-diphenylanthracene, **MANT**, and rubrene all demonstrate a pseudo first order reaction with  $^1\text{O}_2$  (Figure 15). When the

absorbances were plotted against the time exposure to irradiation, a slight curve was exhibited. However, when the  $\ln(\text{absorbance})$  was plotted against the time in seconds, a direct decreasing linear relationship

Conjugated Acene	Rate Constant in $\text{CDCl}_3$	Rate Constant in DCM	Relative Rates in $\text{CDCl}_3$
Rubrene	-0.01185	n/a	11.9
<b>TET</b>	-0.01067	-0.01515	10.7
9, 10 Diphenylanthracene	-0.0011	-0.0008	1.1
<b>MANT</b>	-0.001	-0.0009	1

Table 1. Rate Constants of Conjugated Acenes with Singlet Oxygen. Expanded acenes resulted in ten fold faster rates than the anthracene derivatives.

was demonstrated (Figure 15).

This was predicted for pseudo first order reactions since second order reactions demonstrate a linear relationship when the inverse of the absorbance is plotted against the time. However, an exponential curve is seen

rather than a linear relationship.

This is indicative of the steady state approximation that singlet oxygen concentration is zero order for these reactions, and that the rate is independent of its concentration. Therefore the rate constant observed,  $k_{\text{obs}}$ , is a product of the actual rate constant and singlet oxygen concentration:  $k_{\text{obs}} = k_{\text{act}}[{}^1\text{O}_2]$ . The relative rates are seen in the table below (Table 1). The anthracene derivatives, 9, 10-diphenylanthracene and **MANT**, demonstrate similar reaction rates of endoperoxide formation. However, the expanded conjugated acenes demonstrated a faster reaction rate of approximately ten fold.

## 5, 12-bis(4-methoxyphenyl)tetracene Endoperoxide Formation & Separation

When **TET** is exposed to a solution containing photosensitizer methylene blue and is irradiated, **TET** endoperoxides are formed (Figure 16). The **TET** had two distinguishable protons, shown by the green arrow, at 8.380ppm (Figure 17). After silica column chromatography, two endoperoxides were separated. Each endoperoxide was analyzed by  ${}^1\text{H-NMR}$ . One demonstrated endoperoxide formation at the substituted ring, whereas the second demonstrated the endoperoxide formation at the nonsubstituted ring. The first endoperoxide eluted was distinguishable from the second due to the bridgehead proton peak at 6.059ppm (Figure 17, red arrow). The methyl groups in the two methoxy groups had peaks at 3.965ppm and 3.986ppm, respectively for the first and second endoperoxides.

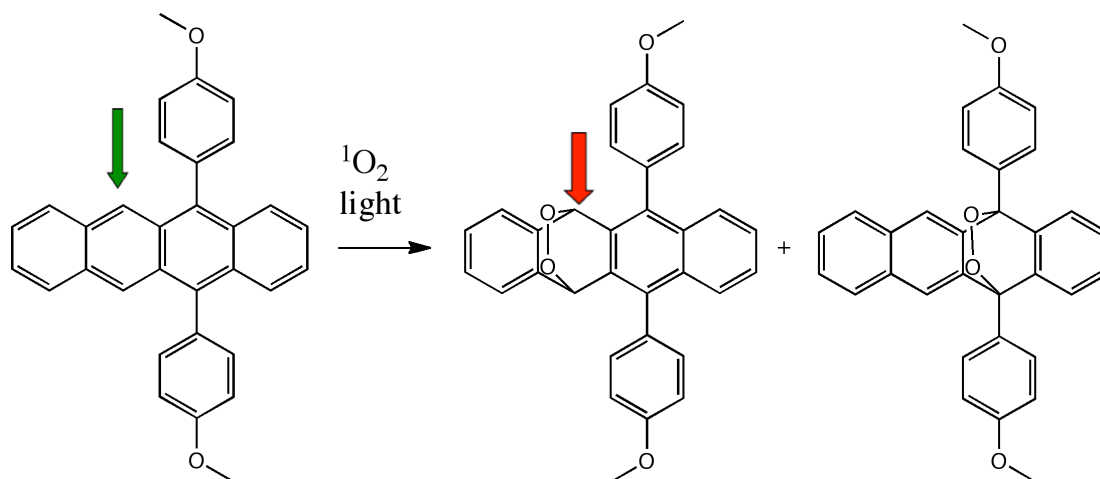


Figure 16. **TET**'s reaction with singlet oxygen results in two forms of endoperoxides, in a ratio of 2:1. These endoperoxides are highly blue shifted in their emission spectra. Singlet oxygen is produced by a photosensitizer upon irradiation.

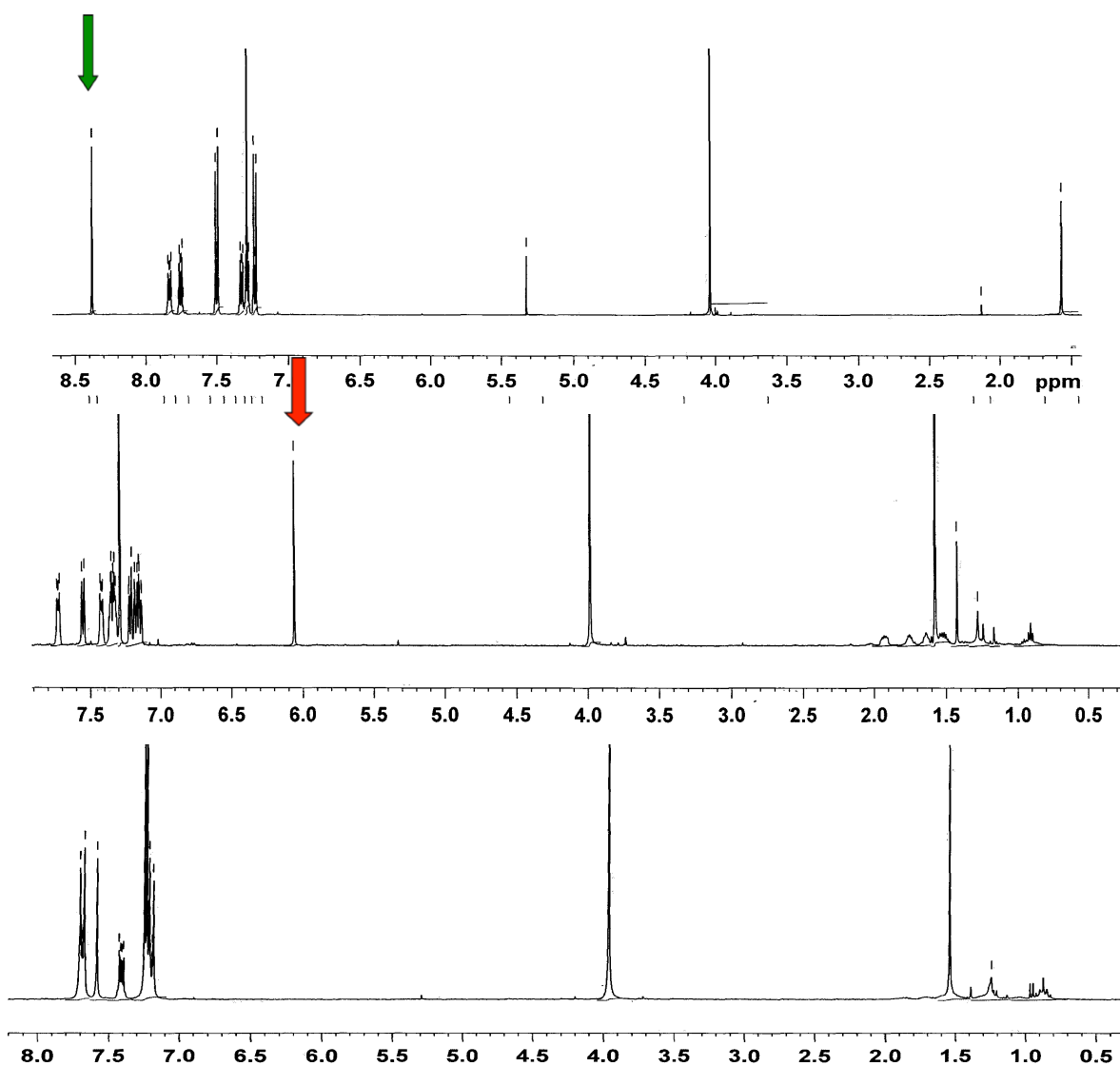


Figure 17. The  $^1\text{H}$  NMR spectra of **TET**, endoperoxide 1, and endoperoxide 2 are shown, top to bottom. The NMR of the first endoperoxide demonstrates a peak at 6.059ppm whereas the second did not.

## Singlet Oxygen Sensor Green Platform for $^1\text{O}_2$ Detection

Singlet Oxygen Sensor Green has the ability to detect singlet oxygen at very low concentrations. Prior to solid phase detection of  $^1\text{O}_2$  with conjugated polymers, this platform was developed to observe if  $^1\text{O}_2$  can indeed be detected in aqueous solution.  $^1\text{O}_2$  was generated with amine reactive eosin 5-isothiocyanate. More specifically, the dye was bound to avidin and biotinylated microspheres. Avidin, a protein found in chicken egg white, contains four identical polypeptide chains that consist of 128 amino acids<sup>12</sup>. Each chain contains a carbohydrate moiety N-linked to an asparagine at residue 17. This glycoprotein has a molecular mass of 67000, in which the carbohydrate moiety is responsible for 10% of the molecular weight of the protein, and is composed of four/five mannose residues and three N-acetyl-glucosamine per chain<sup>12</sup>.

Methylene blue was the singlet oxygen photosensitizer used in the previous experiments; in the following experiments involving protein-dye conjugation, amine reactive eosin 5-isothiocyanate was used. By reacting eosin 5-isothiocyanate with amines on avidin's surface, an **AE** conjugate was prepared. The degree on labeling on this conjugate was determined to be 5.43 eosin molecules per avidin (Appendix Eq 1).

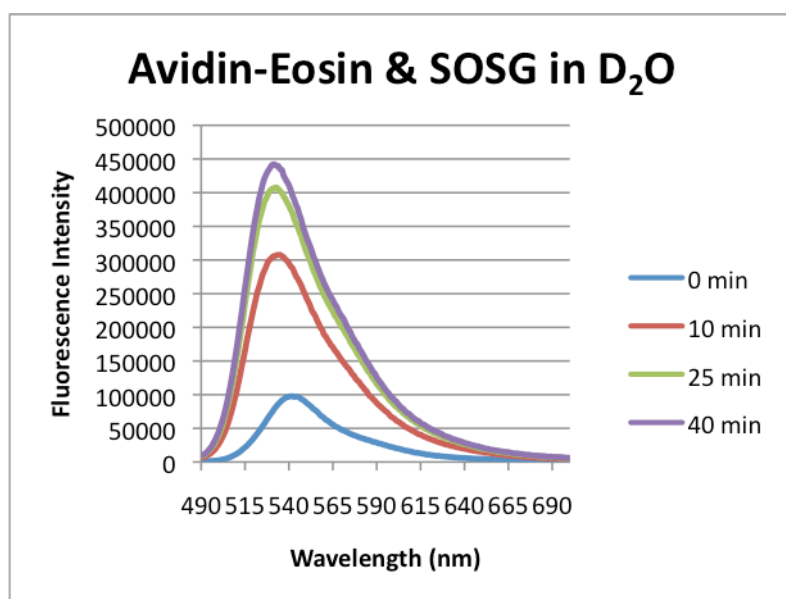


Figure 18. The **AE** complex in a solution of **SOSG**, a singlet oxygen detector, was irradiated with a 435 long-pass filter. The intensity increased 7 fold over the course of 40 min irradiation.

Singlet Oxygen Sensor Green is a commercially available product that is highly specific to singlet oxygen, rather than other reactive oxygen species. Before exposure to singlet oxygen, **SOSG** emits at peaks 395nm and 416nm. However, in the presence of singlet oxygen, **SOSG** emission shifts to emit at peaks 504 and 525 nm. This model was analyzed before replacing **SOSG** as a sensor, since **SOSG** is typically used in aqueous solutions. Therefore, observations of the **AE** complex producing singlet oxygen for **SOSG**

detection were analyzed. When buffered solutions of **SOSG** and **AE** were irradiated with a

435nm long pass filter, constant decreases in the signature peaks of **SOSG** between 300-400 nm were observed. Over time these peaks became less defined, indicating a reaction involving **SOSG** and singlet oxygen was occurring. In the absence of **AE**, **SOSG** showed minimal shifts in its characteristic peaks. However because absorbance was not entirely diagnostic of the reaction, fluorescence was primarily studied to determine more accurate results.

With the **AE** conjugate present with **SOSG** in  $D_2O$ , singlet oxygen production by the eosin 5-isothiocyanate bound to avidin was analyzed (Figure 18). There was initial emission scan displayed an intensity of about 100,000 at 540 nm. However, the fluorescence intensity increased 4.5 times that of the original signal over the course of 40 min of irradiation. This seemed to signify that singlet oxygen was being produced by the eosin 5-isothiocyanate bound to the avidin. The presence of initial peak even in the absence of irradiating the photosensitizer

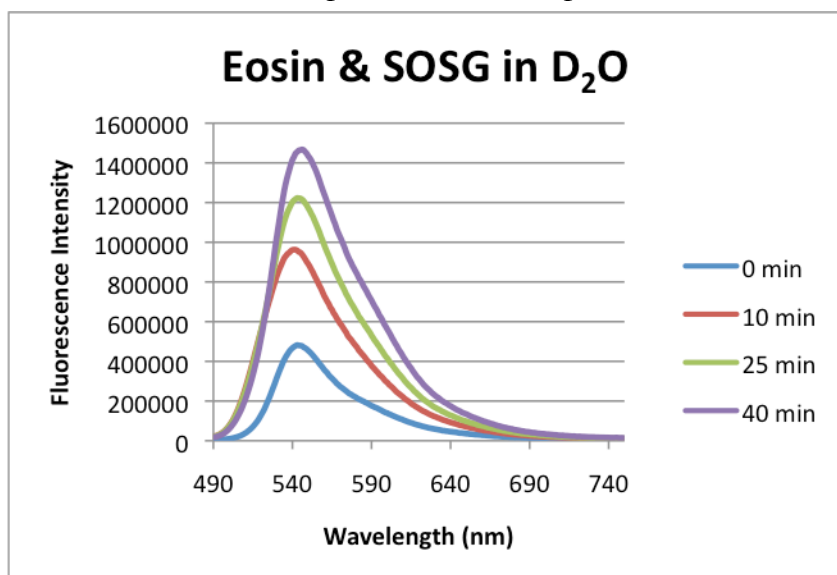


Figure 19. Eosin 5-isocyanate was placed in a solution of **SOSG** and was irradiated to produce singlet oxygen. **SOSG**'s fluorescence increased nearly 3 fold.

indicated that either singlet oxygen was already present within the solution or that **SOSG** demonstrates false initial readings. To determine whether this initial reading was an inherent flaw of **SOSG** or not, several control experiments were performed. Solutions containing **SOSG** were irradiated with light and bubbled with oxygen for saturated oxygen content. When excited at 480nm, **SOSG** exhibited minimal increase in the

fluorescence intensity throughout the experiment. However, the initial fluorescence was rather high at 80,000. In the absence of singlet oxygen photosensitizer, the fluorescence intensity was consistently equal to the initial fluorescence spectrum. No singlet oxygen was produced in the absence of photosensitizer. To determine whether free eosin 5-isothiocyanate produced any singlet oxygen that was detectable by **SOSG**, eosin 5-isothiocyanate was irradiated in the presence of **SOSG** (Figure 19). The initial fluorescent scan had an intensity of around 500,000, peaking around 540 nm. As exposure to light and oxygen increased, the fluorescence intensity increased by 3x the original intensity. As a positive control, another known photosensitizer of

singlet oxygen was irradiated in the presence of **SOSG**. After each exposure to oxygen and light, there was a large increase in the fluorescence. The replacement of AE and eosin 5-isothiocyanate with Rose Bengal demonstrated the effectiveness of **SOSG** as a sensor because **SOSG**'s fluorescence intensity doubled (Figure 18). This indicated that the system was indeed functional as a detector of  $^1\text{O}_2$  as it is being produced, although it has an initial false positive reading. Experiments were initially done in distilled water, though inconsistent spectra were obtained. To improve results, experiments were performed within  $\text{D}_2\text{O}$ . This increased the lifetime of singlet oxygen tenfold from  $2\mu\text{s}$  to  $20\mu\text{s}$ .

In order to determine the specific biochemical binding event, between biotinylated

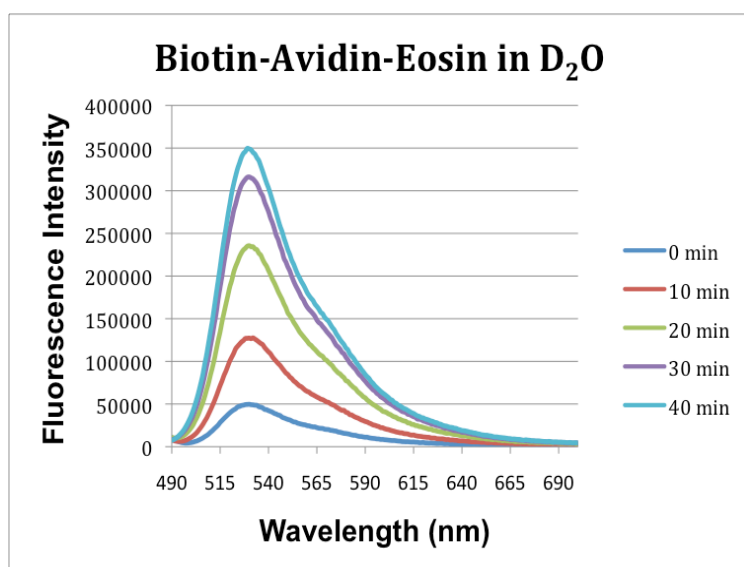


Figure 20. **BAE** in a solution of **SOSG** was irradiated, resulting in a 6 fold increase of **SOSG**'s fluorescence.

microsphere and the avidin-eosin conjugate, and whether singlet oxygen is efficiently produced to create a response in **SOSG**, avidin-eosin was bound to biotin. The avidin-biotin complex is a prevalent immunocytochemical technique that is highly sensitive and specific. To prepare the analyte, the antigen is recognized initially by a primary antibody<sup>13</sup>. A secondary antibody, conjugated with biotin, is then bound to the first antibody. In a separate reaction, biotin and avidin are mixed in a

ratio to leave unoccupied binding sites on the avidin. The biotin-avidin complex can then bind in order for detection to occur<sup>9</sup>. Essentially, avidin contains four potential binding sites for biotin<sup>9</sup>. One substrate site binds to the biotin on the secondary antibody while the other three sites bind to free biotin. This method can be used for analyte detection through the antibody-biotin conjugate.

To observe whether the specific interactions between **AE** and biotin produced singlet oxygen, biotinylated microspheres were attached to the **AE** complex. This **BAE** complex was placed in a solution of **SOSG** and irradiated. As previously seen, the initial fluorescence intensity of the solution was approximately 50,000 (Figure 20). Over the course of the reaction, the fluorescence intensity increased 6 fold, indicating that there was a significant increase in signal

due to singlet oxygen production from the eosin 5-isothiocyanate bound to **BAE**. To fully

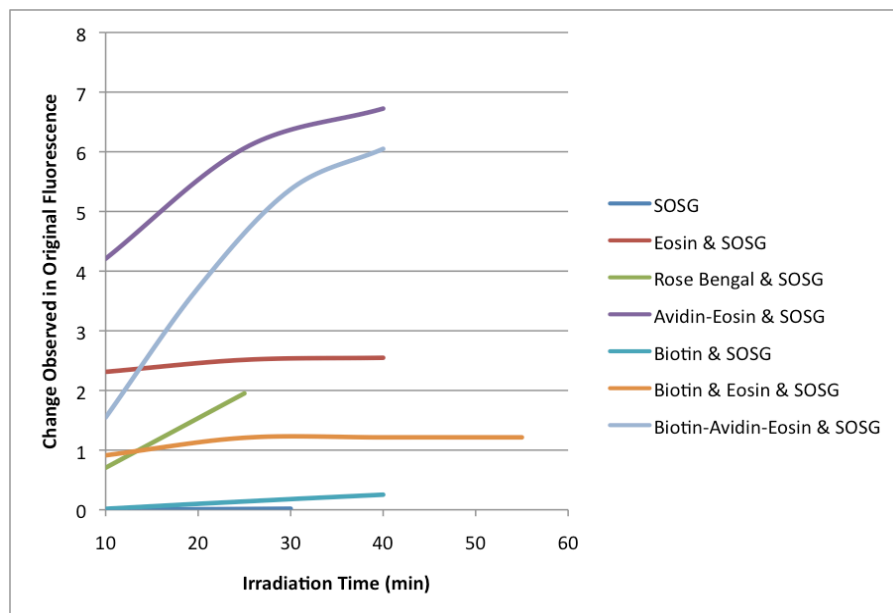


Figure 21. The change in **SOSG**'s fluorescence when exposed to various control and experimental solutions is shown. Solutions lacking photosensitizer resulted in insignificant changes in fluorescence.

attribute this increase to the **BAE** complex, two controls were performed. When washed biotinylated microspheres were placed in a solution of **SOSG**, a very slight increase in fluorescence was detected. In comparison to the **BAE** complex, this change in fluorescence was indeed negligible (Figure 21). A second control involved placement of biotinylated microspheres with amine reactive eosin and **SOSG**.

This produced an increase in fluorescence, which demonstrated

that eosin 5-isothiocyanate has the ability to photosensitize  $^1\text{O}_2$  in the presence of biotinylated microspheres (Figure 21). These two control experiments reveal that the specific binding event of biotinylated microspheres to an **AE** complex generates  $^1\text{O}_2$  that is detectable by **SOSG**.

Initially, spectrophotometry was used to detect **SOSG** as  $^1\text{O}_2$  was being generated, although these measurements were not as diagnostic of the singlet oxygen generation as fluorescence. This was primarily due to the scattered light typically associated with solid containing samples.

### **TET:PF Thin Film Detection of $^1\text{O}_2$**

**TET** is a highly fluorescent molecule, whose extinction coefficient and quantum yield are approximately  $8776 \text{ M}^{-1} \text{ cm}^{-1}$  and 0.61, respectively (Appendix Eq 3). Its emission spectrum overlaps significantly with the conjugated polymer, **PF**'s absorption spectrum. This overlap indicated the potential of energy transfer from the **PF** to **TET** through resonance energy transfer. Resonance energy transfer RET occurs when the emission spectrum of a fluorophore overlaps with the absorption spectrum of the acceptor, which is not required to fluoresce, due to noncovalent interactions<sup>11</sup>. Energy transfer occurs when the donor emits at shorter wavelengths that overlap with the acceptor's absorption spectrum. This occurs through long-range dipole dipole interactions and the rate of energy transfer depends on the amount of overlap between

these two spectrums, the distance between the donor and the acceptor, and the donor's quantum yield. Essentially, the fluorophore has an oscillating dipole that has the ability to exchange energy with another dipole with similar resonance frequencies. In the case where the acceptor, such as **PF**, is fluorescent, the energy transfer enhances the acceptor's emission. The efficiency of energy transfer from the donor to the acceptor determines the distance between the two. The

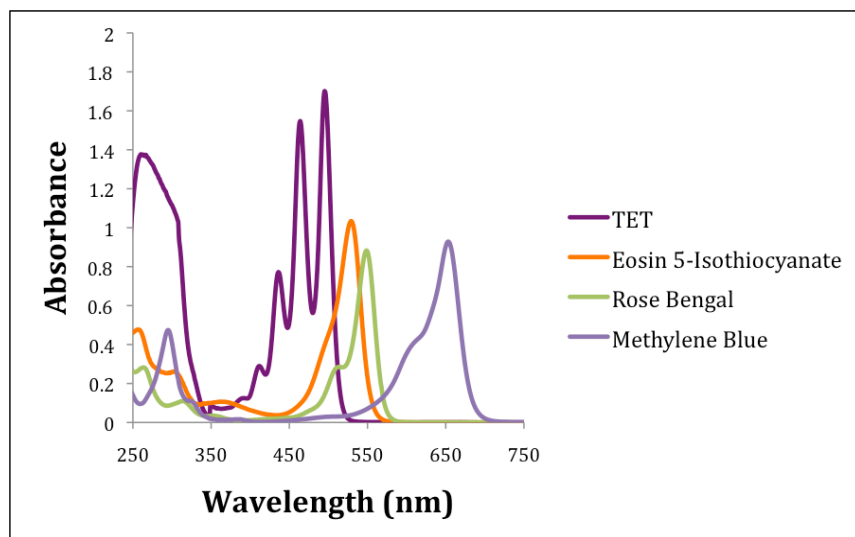


Figure 22. The absorption of three photosensitizers are shown in comparison to that of **TET**. Methylene Blue is highly red shifted and distinct from that of **TET**, whereas the other two have considerable overlap with **TET**.

distance in which the energy transfer is 50% efficient, Forster distance, is around 20-60 angstroms. The rate of this energy transfer is calculated by  $k_T = 1/\tau_D (R_0/r)^6$  where  $\tau_D$  is the decay time of the donor,  $R_0$  is the Forster distance, and  $r$  is the distance between the donor and acceptor. The rate of energy transfer is inversely proportional to  $r^6$ . Because the energy transfer rate is so heavily dependent on the distance between the donor and acceptor, any phenomenon that alters

this distance will affect the energy transfer as well. The solid state interactions do not require the conjugated polymer to be bound to the tetracene pendants for energy transfer to occur. For this reason, when a solution of **PF** and **TET** were spin coated onto a thin film, the proximity and interlay of the two molecules allowed for efficient energy transfer. Because of the efficiency of exciton mobility of the **PF**, small amounts of **TET** can fully quench the **PF**'s fluorescence. For unlinked donor-acceptor energy transfer, the acceptor is present in millimolar concentration so that the acceptor molecules are within the Forster distance from the donor.

However, **TET**'s quenching ability can be closed down through a [4+2] cycloaddition with singlet oxygen, which is produced by a photosensitizer (Figure 22). It is crucial that tetracene react quickly with the short lived singlet oxygen in order for this Diels Alder reaction to occur. Upon reaction with singlet oxygen, **TET**'s quenching slows significantly simultaneously restoring the conjugated polymer's fluorescence. The endoperoxides that result are blue shifted away from the **PF**'s emission; hence, energy transfer pathways are interrupted.

By observing the **TET**'s fluorescence intensity at its maximum wavelength 510nm and **PF**'s maximum intensity at 420nm, a ratiometric shift can be observed (Appendix Eq 4). This ratiometric change that is observed is greatly advantageous.

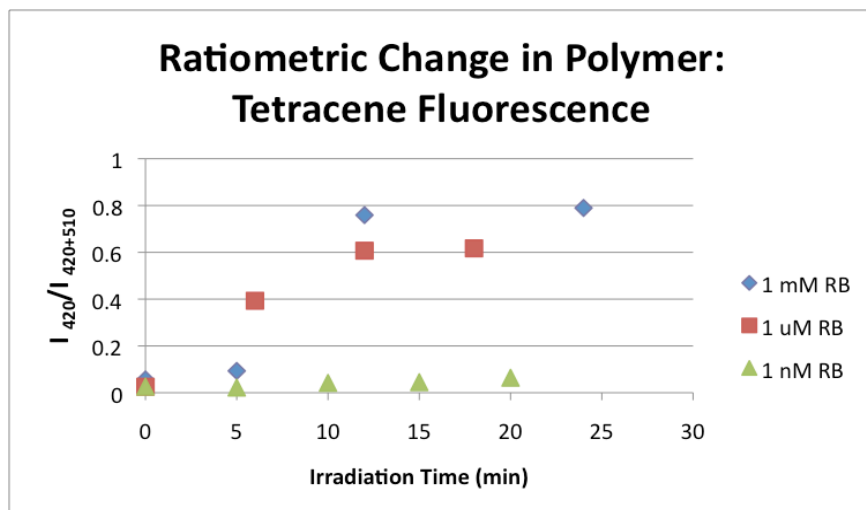


Figure 23. Various concentrations of **RB** were used to detect a ratiometric shift in the **TET:PF** fluorescence. The 1nM **RB** produced no significant shift.

### 10% **TET/PF** Film with a 515 Band Pass Filter with Varying **RB** Concentrations

An initial experiment involved exposing the 10% **TET:PF** film to Rose Bengal in distilled water before the film's placement in front of the lamp. Since droplets from the Rose Bengal solution

remained on the film while irradiation, singlet oxygen was

generated. This was observed by the simultaneous decreasing **TET** intensity and increasing **PF** intensity. In order to increase the exposure to singlet oxygen, the film was placed in distilled water containing **RB** while synchronized to light exposure. The Rose Bengal concentration was varied to distinguish the lower limit of detection of the **PF**'s restored fluorescence. Rose Bengal concentrations of 1mM, 1μM, and 1nM resulted in a ratiometric shift from **TET** to **PF** (Figure 23). However, 1nM Rose Bengal did not produce significant singlet oxygen for a Diels Alder reaction to occur. To determine if **TET**'s quenching was altered by reacting with singlet oxygen, various negative controls were also performed.

Multiple scans of the film were taken before and after exposure to UV light in distilled water; different tetracene fluorescence spectra with each measurement was observed after exposure of a 10% **TET:PF** film to UV light filtered with a 515nm colored glass filter (Figure 23). This was due to the varying fluorophore concentrations present within each area of the film that was excited by the fluorimeter. Areas with more **TET** molecules would result in higher intensities after each scan whereas areas with lower **TET** concentrations would result in lower intensity scans. The difference in **TET**'s fluorescence of each spectra can be attributed to the difference in light intensity hitting the sensor from each exposed area on the film or the

decomposition of the tetracene. Each exposure resulted in a unique tetracene fluorescence but showed no significant fluorescence intensity for the polymer. The rotation of the film supported

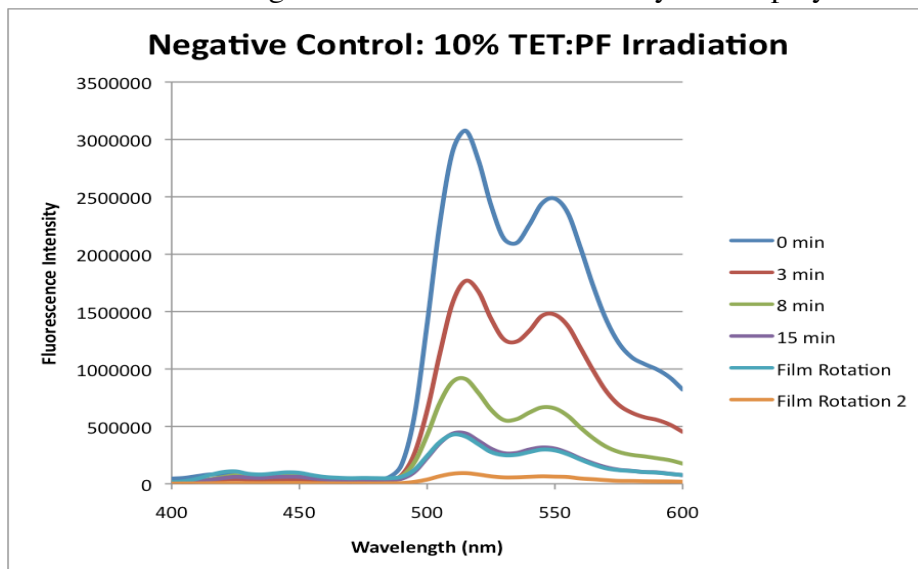


Figure 24. Variations in **TET**'s fluorescent intensities are shown when irradiated in aqueous solution containing no photosensitizer. No **PF** fluorescence is shown.

the spontaneity of the film's tetracene fluorescence. Because the ratiometric relationship requires the polymer fluorescence to increase while the **TET** fluorescence simultaneously decreases, no reaction occurred. This experiment demonstrated the requirement of a photosensitizer in the production of singlet oxygen since tetracene did not self

sensitize singlet oxygen in order to stop **TET** from quenching the polymer.

As a second negative control, the film was placed in distilled water for 1 min before being irradiated with light using the 515 nm filter. Similarly, fluorescent scans were taken before and after each exposure. There was no significant change in the polymer's fluorescence. A third negative control involved the film's exposure to photosensitizer Rose Bengal in distilled water for 1 min intervals in the absence of UV light exposure. This control signified the importance of exposing Rose Bengal to light in order to generate singlet oxygen. As previously mentioned, the tetracene is not a sufficient photosensitizer of singlet oxygen; two crucial components to the **TET:PF** system were the presence of a photosensitizer as well as exposure of the photosensitizer to light.

### 10% **TET: PF** Film with Varying Filters

Due to the considerable overlap of **TET**'s UV absorption with Rose Bengal's UV absorption, the **TET** moieties are exposed to UV-light using the 515nm filter (Figure 22). To avoid tetracene degradation for proper energy transfer and to distinguish the extent of the energy transfer previously observed from degradation of **TET**, two other filters were utilized (Figure 25). A 570nm colored filter was used while exposing the film to  $1\mu\text{M}$  Rose Bengal solution since

**TET** shows no absorbance past 570nm. Since Rose Bengal absorbs considerably less after 570 nm, the Diels Alder reaction occurs much slower compared with a 515nm filter since singlet oxygen is being generated much slower. A second reaction was performed increasing the RB concentration by a factor of ten, similar results were obtained. To accommodate maximum

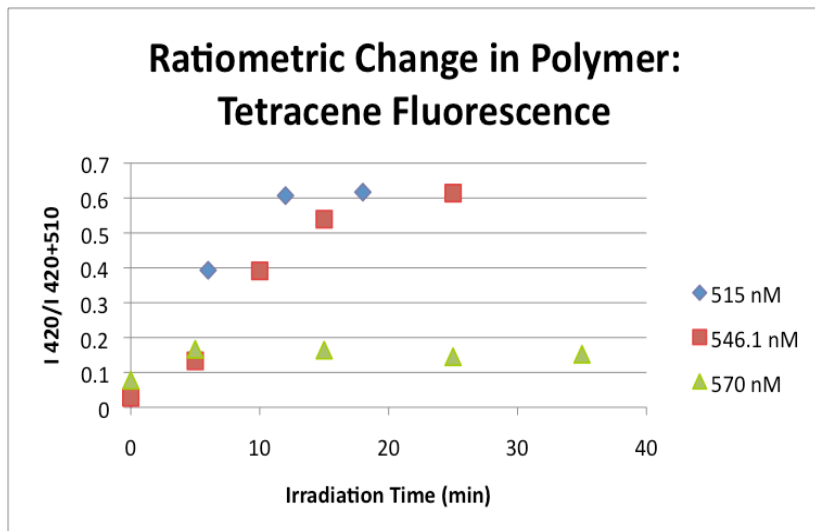


Figure 25. A 515nm long-pass filter, 546.1nm band-pass interference filter, and a 570nm long-pass filter were used to isolate RB for irradiation.

absorption by Rose Bengal while avoiding any **TET** degradation, a band-pass interference filter of 546.1nm was then employed while irradiating the 10% film without Rose Bengal. This negative control did not cause a ratiometric shift as earlier shown with the 515nm filter. In a solution of 10 $\mu$ M Rose Bengal, the film demonstrated increasing polymer fluorescence intensity while

decreasing the tetracene's fluorescence intensity. Long pass filters, such as the 515nm and 570nm filter, cut on at specific wavelengths to allow for high transmittance at 50% of peak transmission<sup>13</sup>. The 515nm and 570nm filters are colored filter glass, or absorption glass<sup>14</sup>. These filter types controls transmittance solely based on absorption. Therefore, the thickness of the glass is correlated to the blocking level of light<sup>14</sup>. The 546.1nm filter was a bandpass filter with a center wavelength at 546.1nm and a bandwidth of 10.0nm. It was evident that the 570nm filter resulted in lower ratiometric shifts compared to either the 515nm filter or 546.1nm filter. This was most likely due to slower kinetics as previously mentioned. Likewise, the 546.1nm filter appeared to shift the film's fluorescence, through the production of singlet oxygen, at a slightly slower pace than the 515nm filter. The 546.1nm filter corresponded to a .4 ratiometric shift at 10min of irradiation, while the 515nm filter resulted in a .4 ratiometric shift at 6 min. Nonetheless, the 546.1nm filter produced singlet oxygen at an acceptable rate to monitor the fluorescence shift from **TET** to **PF**.

### Varying Percentages TET:PF Films with a 546.1 nm Filter in 1 $\mu\text{M}$ RB/ D<sub>2</sub>O

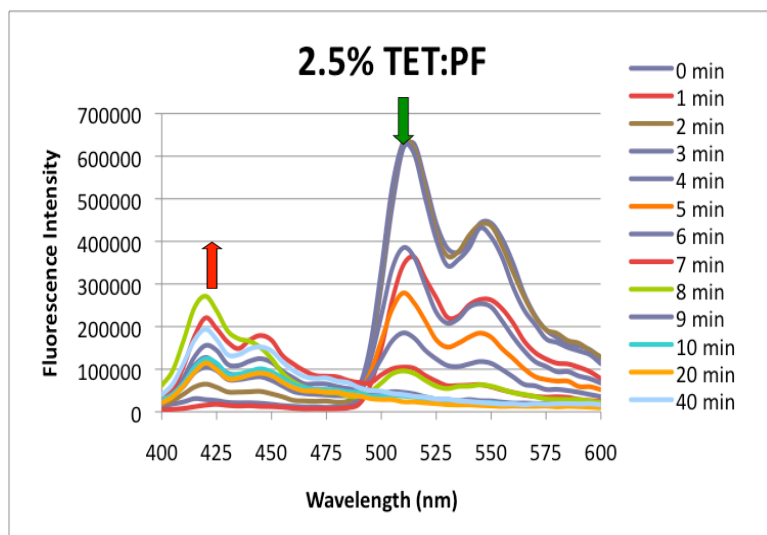


Figure 26. As exposure to singlet oxygen, via irradiation of **RB**, increased, the **TET:PF** fluorescence changes. The **TET** fluorescence at 510nm decreases, while the **PF** fluorescence at 420nm increases.

of the ratio between the concentrations of **TET** and poly(fluorene), 1%, 2.5%, and 10% **TET:PF** films were prepared through dilution (Figure 26). These films were exposed to a 1  $\mu\text{M}$  **RB**/ D<sub>2</sub>O solution while irradiate with UV light with a 546.1nm filter. Each film type approached a

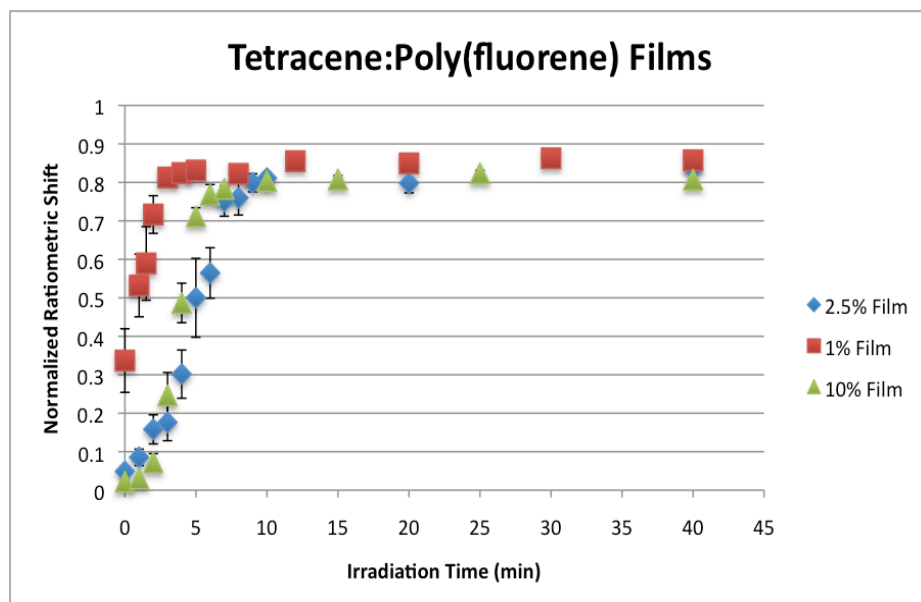


Figure 27. The ratiometric shifts of a 1%, 2.5%, and 10% **TET:PF** films are shown. The 1% film demonstrates initial **PF** fluorescence, while the 2.5% film demonstrated less of an induction period than the 10% film.

Because energy transfer is typically independent of any solvent and the orientation of donor and acceptor molecules, a solution of distilled water was initially used<sup>11</sup>. However, to increase the lifetime of singlet oxygen by a factor of 10, deuterium oxide was used to create all Rose Bengal solutions. This closed down the energy transfer pathway efficiently since it allowed more <sup>1</sup>O<sub>2</sub> to interact with the

**TET:PF** film. To examine the effect

normalized ratiometric shift of approximately .85. The 1% film displayed insufficient quenching of the **PF** (Figure 27). Before any exposure to light and **RB**, the film should display no polymer fluorescence. However, the 1% film demonstrated an average initial fluorescence of 0.32 with the higher and lower limits of 0.25 to 0.42. The low **TET:PF** ratio indicated that a higher tetracene concentration is required to accurately be applied as a

biosensor. This initial ratiometric shift prior to exposure to the photosensitizer or light was similar to the initial fluorescence of **SOSG** prior to any necessary exposures. The 10% **TET:PF** films demonstrated a sigmoidal type curve that indicates the presence of an early induction period. During this period, singlet oxygen reactions with **TET** produce no significant shift in the polymer's fluorescence. There is therefore a critical concentration of endoperoxides that are formed that allows restoration of the **PF**'s fluorescence. At low analyte levels, it is important that the film produces a response with every exposure to singlet oxygen. The 2.5% film displayed smaller shifts away from **TET**'s fluorescence. This film also displayed less dramatic ratiometric changes as compared to the 10% film. The slight changes with each exposure that the 2.5% film produces, allows it to be a platform for future biosensing assays.

### 2.5% **TET: PF** Films with a 546.1 nm Filter in Varying **RB** Concentrations

To determine the lowest concentration of Rose Bengal that is necessary to induce a reaction between **TET** and singlet oxygen, a 2.5% **TET:PF** film was placed in several differing

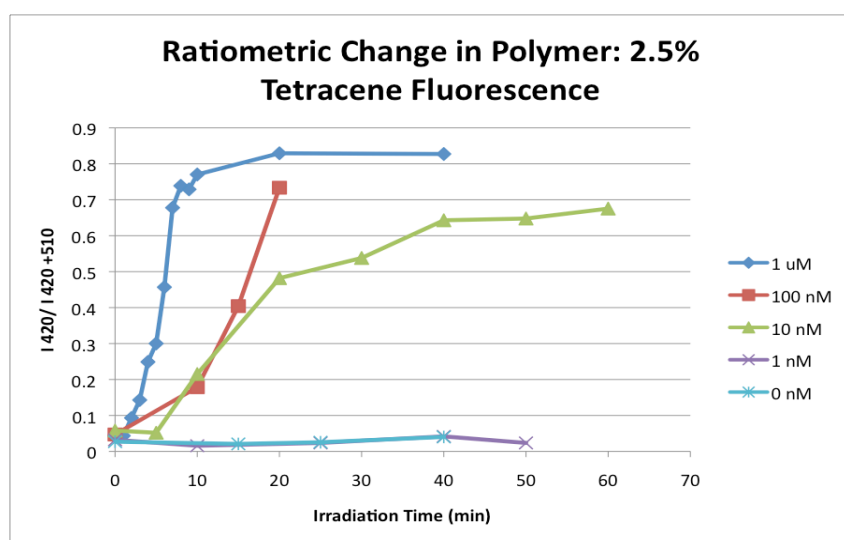


Figure 28. Various concentrations of **RB** were used to analyze the ratiometric shift of a 2.5% **TET:PF**. The 1  $\mu$ M **RB** demonstrated a faster response compared to other concentrations; the 1 nM **RB** produced no significant shift.

**RB** solutions. In addition to the 1  $\mu$ M **RB/ D<sub>2</sub>O** solutions tested, multiple solutions of 100 nM, 10 nM, and 1 nM **RB/ D<sub>2</sub>O** were analyzed (Figure 28). With the exception of 1 nM **RB/ D<sub>2</sub>O**, each produced a significant ratiometric shift up to 0.70. The 1 nM **RB/ D<sub>2</sub>O** indicated no alteration from the original tetracene fluorescence. A negative control experiment was also performed that resulted in no significant ratiometric shifts as the 1 nM **RB** solution. This indicated that

the 2.5% **TET:PF** film was able to sufficiently detect the presence of **RB** as low as 10 nM. **TET** degradation was minimized by using the 546.1 nm band pass filter. After each round of exposure to Rose Bengal and light, the fluorescence of the **TET** decreased over time, while the fluorescence of the polymer increased. More importantly, the ratio of the polymer's fluorescence intensity to that of the tetracene increased over time.

## 2.5% TET/PF Films & Biotinylated Microspheres Bound to NeutrAvidin/Eosin 5-isothiocyanate

To develop platform to indicate that a specific biochemical binding event produces these results as well, biotinylated microspheres were attached with avidin through specific binding. The avidin/biotin bond is incredibly strong, allowing an ideal system for affinity binding. Avidin, however, can result in nonspecific interactions with negatively charged ligands due to its overall positive charge at neutral pH (pI of 10); this can be improved by using streptavidin, which has a net negative charge at neutral pH (pI of 5), has reduced non specific interactions. The avidin is then bound to a singlet oxygen photosensitizer in order to produce singlet oxygen during

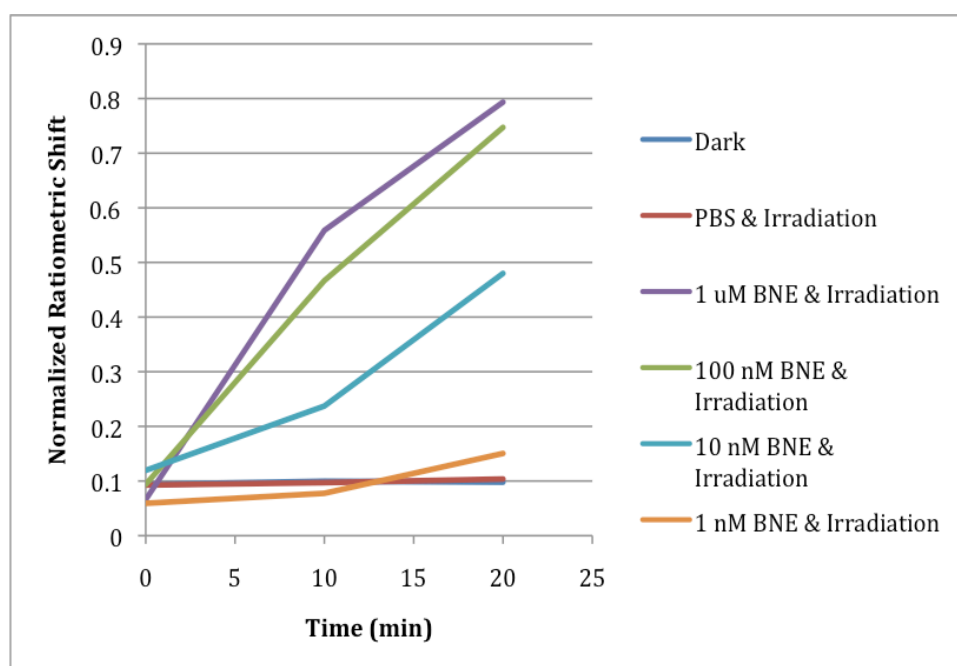


Figure 29. Various concentrations of **BNE** were irradiated using a 530nm long-pass filter. The 1 $\mu$ M, 100nM, and 10nM produced a considerable shift in the **TET: PF** fluorescence. The 1nM **BNE**, 0nM, and dark solutions produced insignificant shifts.

irradiation. To eliminate any nonspecific binding from the avidin, NeutrAvidin was used to improve selective binding with biotin-coated microspheres. NeutrAvidin is a modified form of avidin without the carbohydrate attachments. By using NeutrAvidin rather than avidin, nonspecific interactions due to the carbohydrates are reduced. It is important to note that the photosensitizer is therefore bound to the biotin via the

protein. Any free protein is not exposed to the conjugated polymer to avoid any non-specific interactions between the two. This method appears to produce singlet oxygen that is reactive with the hydrophobic film.

2.5% **TET:PF** films were placed in various concentrations of NeutrAvidin-Eosin 5-isothiocyanate complexes bound to biotinylated microspheres and were irradiated with a 530nm long pass filter. The 530 filter reduced any absorption of light by the **TET** rather than the eosin 5-isothiocyanate because **TET**'s absorption is minimal at 530nm (Figure 22). These experiments

involved two fluorescent scans in order to limit any **TET** degradation from the emission scan. It can be seen that the irradiated  $1\mu\text{M}$  and  $100\text{nM}$  **BNE** solutions resulted in dramatic ratiometric shifts, whereas both the dark and PBS only solutions resulted in no significant shift (Figure 29). A second set of experiments with  $10\text{nM}$  **BNE** demonstrated that at approximately 45min of irradiation, the resulting ratiometric shift was as high as 0.80, indicating that the acene reaction occurred at a slower rate. Previous experiments using the 515nm filter in a control PBS solution demonstrated ratiometric shifts, most likely corresponding to **TET** degradation, up to 0.4 even in the absence of photosensitizer.

This project required several control experiments to demonstrate the mechanism's

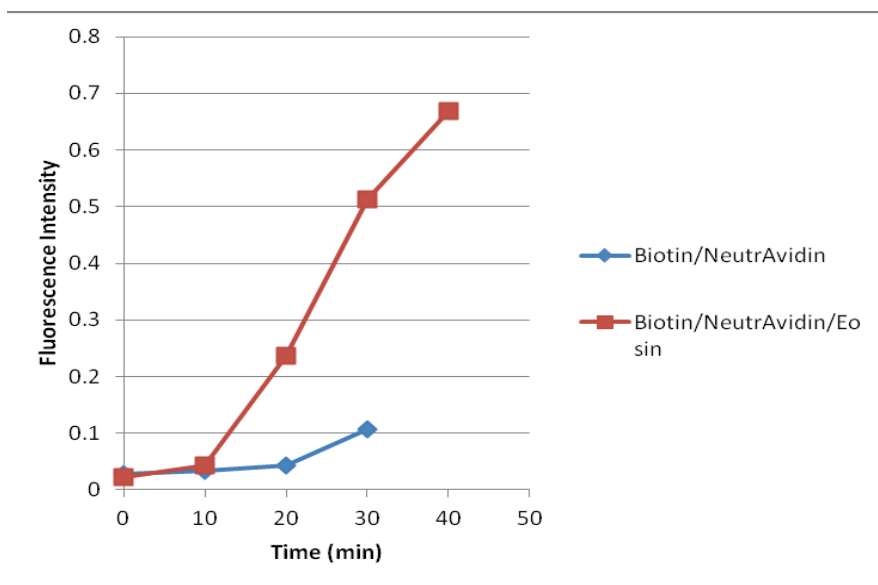


Figure 30. The protein-biotinylated microspheres produced a small fluorescent shift on the 2.5% **TET:PF** film, whereas the protein-dye-biotinylated microspheres demonstrated a large fluorescent shift.

accuracy. In a reaction that involved non-biotinylated beads, there would be no binding to the avidin-eosin conjugate, resulting in no change in conjugated polymer's fluorescence. Two main negative control experiments were therefore performed to demonstrate that it is the specific interaction between biotinylated microspheres and the NeutrAvidin/eosin 5-isothiocyanate complex that generates singlet oxygen, which is detected by the **TET:PF** film.

Firstly, NeutrAvidin was attached to biotinylated microspheres and irradiated with a 530nm filter. Compared to the **BNE** complex, the complex without the photosensitizer produced a much lower level of response (Figure 30). This was indicative that the amine reactive eosin was responsible for the larger ratiometric shift in the **TET:PF** film. Lastly, a solution of non-functionalized polystyrene microspheres were reacted with the NeutrAvidin/eosin 5-isothiocyanate in a PBS buffer and a 1% BSA doped PBS buffer. It appeared that the 1% BSA work up decreased nonspecific interactions with the protein-dye complex, which resulted in lower ratiometric shifts of approximately 0.3 when compared to a non BSA work up, a shift of approximately 0.5 after 40 min of irradiation.

## Conclusion

This project demonstrated that multiplicative amplification was possible using singlet oxygen and conjugated polymers in aqueous solutions. The **SOSG** model used with the **AE** complex bound to biotinylated microspheres demonstrated a high fluorescence increase by 7 fold. However, initial fluorescence was present in the absence of singlet oxygen generation. This was improved by using a **TET:PF** thin film, in which **TET** quenches **PF** fluorescence. A nearly complete ratiometric shift from the **TET** to **PF** fluorescence was observed when the photosensitizer, **RB**, was irradiated and produced  $^1\text{O}_2$ . The lowest concentration of **RB** that produced singlet oxygen to react with the film was 10nM. When **BNE** replaced **RB**, the results indicated that there was still tetracene degradation. This may be improved by using a 550nm long pass filter to completely avoid absorption by **TET**. However, this does compromise the rate of the ratiometric shift. Perhaps synthesis of an amine reactive photosensitizer with a more red shifted absorption would allow for quick singlet oxygen generation while completely isolating the photosensitizer during irradiation. Coupled with a 550nm filter, using BSA to minimize non specific interactions may improve the control's fluorescent spectra. A longer objective is to synthesize a hydrophilic CP, with acene moieties, that is readily water soluble and reflects the ratiometric response seen with the thin films.

Nonetheless, the acene doped **PF** film demonstrated a change in fluorescence in the presence of singlet oxygen. As compared to the **SOSG** model, this system allows for internal referencing through the use of wavelength ratiometric measurements. This method also prevents the protein-dye complex by directly interacting with the thin film to produce a response. Rather, a second analyte, which requires irradiation, is used for specific interactions with the acenes. This can be applied to many bioanalytical applications since there will be no impediments raised by the presence of large proteins. This is because singlet oxygen transduces the presence of the biomolecule. It has the ability to improve non-specific bindings between the conjugated polymer and protein, resulting in more reliable and accurate quantitative measurements.

## Appendix

### Equation 1: Avidin-Eosin 5-isothiocyanate Degree of Labeling

The protein concentration was determined using the following equation Protein Concentration (M) =  $[A_{280} - (A_{525} * .29)] / \epsilon = A_{\text{protein}} / \epsilon$  where 0.29 is the correction factor,  $A_{280}$  is the absorbance at 280 nm,  $A_{525}$  is the absorbance at 525 nm, and  $\epsilon$  is the extinction coefficient of avidin.

$$\text{Protein Concentration (M)} = [1.42633116 - (2.16630578 * 0.29)] \text{ cm}^{-1} / 1800000 \text{ cm}^{-1} \text{ M}^{-1} = 4.4339 * 10^{-6} \text{ M}$$

The degree of labeling was determined using the following equation  $\text{DOL} = A_{525} / (\epsilon * [\text{protein}])$  where  $\epsilon$  is the extinction coefficient of eosin at 525 nm.

$$\text{DOL} = 2.16630578 \text{ cm}^{-1} / (90000 \text{ cm}^{-1} \text{ M}^{-1} * [4.4339 * 10^{-6} \text{ M}]) = 5.43$$

### Equation 2: NeutrAvidin-Eosin 5-isothiocyanate Degree of Labeling

The protein concentration was determined using the following equation Protein Concentration (M) =  $[A_{280} - (A_{525} * 0.29)] / \epsilon = A_{\text{protein}} / \epsilon$  where 0.29 is the correction factor,  $A_{280}$  is the absorbance at 280 nm,  $A_{525}$  is the absorbance at 525 nm, and  $\epsilon$  is the extinction coefficient of avidin.

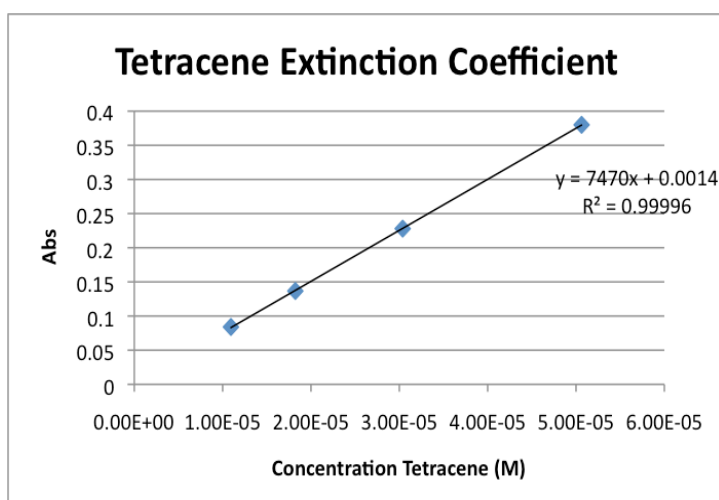
$$\text{Protein Concentration (M)} = [2.96359539 - (3.97375631 * 0.29)] \text{ cm}^{-1} / 166000 \text{ cm}^{-1} \text{ M}^{-1} = 1.09109 * 10^{-5} \text{ M}$$

The degree of labeling was determined using the following equation  $\text{DOL} = A_{525} / (\epsilon * [\text{protein}])$  where  $\epsilon$  is the extinction coefficient of eosin at 525 nm.

$$\text{DOL} = 3.97375631 \text{ cm}^{-1} / (90000 \text{ cm}^{-1} \text{ M}^{-1} * [1.09109 * 10^{-5} \text{ M}]) = 4.05$$

### Equation 3: 5, 12-bis(4-methoxyphenyl)tetracene Quantum Yield & Extinction Coefficient

Extinction coefficient, or molar absorptivity, is an intrinsic property of how strongly molecules absorb light. The extinction coefficient of the tetracene was determined to have an average of



8776  $\text{M}^{-1} \text{ cm}^{-1}$ . The wavelength 495nm was used since the absorption of characteristic tetracene peak was at its maximum. The quantum yield is the number of photons emitted relative to the number of photons absorbed.  $\Phi = \text{number of photons emitted} / \text{number of photons absorbed}$ . The maximum quantum yield is 1, which results when

every photon absorbed is emitted thereafter. **TET**'s quantum yield was calculated using the standard Coumorin 6, which is known to have a well known quantum yield of 0.78. The equation was used to calculate tetracene's quantum yield:  $\Phi_{\text{TET}} =$

$\Phi_{\text{REF}}(I_{\text{TET}}/I_{\text{REF}})(OD_{\text{REF}}/OD_{\text{TET}})(n_{\text{TET}}^2/n_{\text{REF}}^2)$  where  $\Phi_{\text{TET}}$  is the quantum yield of the tetracene,  $\Phi_{\text{REF}}$  is Coumorin 6's quantum yield,  $I_{\text{TET}}$  is the total emission intensity of the tetracene,  $I_{\text{REF}}$  is the total emission intensity of Coumorin 6,  $OD_{\text{TET}}$  is the absorbance of tetracene at 435nm,  $OD_{\text{REF}}$  is the absorbance of Coumorin 6 at 435nm,  $n_{\text{TET}}$  is the refractive index of the solvent tetracene was dissolved in (DCM), and  $n_{\text{REF}}$  is the refractive index of the solvent Coumorin 6 was dissolved in (EtOH). Therefore, the **TET** quantum yield calculation was

$\Phi_{\text{TET}} = 0.78(39308320.91/81469688.19)(.05629145/.036458265)(1.424^2/1.36^2) = 0.64$ . The average quantum yield calculation of tetracene was determined to be 0.61. The wavelength 435nm was used for OD values because both tetracene and Coumorin 6 had a significant absorbance at this wavelength.

#### Equation 4: Normalized Ratiometric Shift

This normalized ratiometric shift compares the maximum fluorescence intensity (I) of **TET** at 510 nm to that of the **PF** at 420nm. The equation accounts for the varying tetracene intensities, as well as the varying polymer intensities while relating the ratio between each. The equation is Normalized Ratiometric Shift =  $I_{420}/(I_{420} + I_{510})$ .

#### References

<sup>1</sup> Dwight, SJ, et al. "Perturbation of fluorescence by nonspecific interactions between anionic poly(phenylenevinylene)s and proteins: implications for biosensors." *J Am Chem Soc.* 126.51 (2004): 16850-16859. <<http://www.ncbi.nlm.nih.gov/pubmed/15612724>>.

<sup>2</sup> Thomas, Samuel W III, et al. "Chemical Sensors Based on Amplifying Fluorecent Conjugated Polymers." *Chem. Rev.* 107 (2007):1339-1386. <<http://web.mit.edu/tswager/www/Papers/213-ChemRev.pdf>>.

<sup>3</sup> He, Fang, et al. Fluorescent Amplifying Recognition for DNA G-Quadruplex Folding with a Cationic Conjugated Polymer: A Platform for Homogeneous Potassium Detection *Journal of the American Chemical Society* 127.35 (2005):12343-12346. <<http://pubs.acs.org/action/showCitFormats?doi=10.1021%2Fja051507i>>.

- <sup>4</sup>Li, Chun, et al. "Unexpected Chiroptical Inversion Observed for Supramolecular Complexes Formed between an Achiral Polythiophene and ATP." *Chemistry-An Asian Journal*. 1.1-2 (2006):95-101. <<http://onlinelibrary.wiley.com/doi/10.1002/asia.200600039/full>>.
- <sup>5</sup>Gaylord, Brent S., et al. "DNA Hybridization Detection with Water-Soluble Conjugated Polymers and Chromophore-Labeled Single-Stranded DNA." *J Am Chem Soc*. 125.4 (2003):896-900. <<http://pubs.acs.org/doi/abs/10.1021/ja027152%2B>>.
- <sup>6</sup>You, MingXu, et al. Fluorescent detection of singlet oxygen: Amplifying signal transduction and improving sensitivity based on intramolecular FRET of anthryl appended porphyrins." *Chinese Science Bulletin*. 56.31 (2011):3253-3259.  
<<http://www.springerlink.com/content/t18563250383358k/fulltext.pdf>>.
- <sup>7</sup>Reddy, Ravikumar and Michael Bendikov. "Diels–Alder reaction of acenes with singlet and triplet oxygen – theoretical study of two-state reactivity." *Chem. Commun.* (2006):1179-1181.  
<<http://pubs.rsc.org/en/content/articlepdf/2006/cc/b513597d>>.
- <sup>8</sup>Umezawa, Naoki, et al. "Novel Fluorescent Probes for Singlet Oxygen." *Angewandete Chemie International Edition*. 38.19 (1999):2899-2901. <<http://www.ncbi.nlm.nih.gov/pubmed/10540386>>.
- <sup>9</sup>Petersen, Signe Beck, et al. "Comparison of a Luminescent Oxygen Channeling Immunoassay and an ELISA for detecting Insulin Aspart in human serum." *Journal of Pharmaceutical and Biomedical Analysis*. 51.1 (2010):217-224. <<http://www.sciencedirect.com/science/article/pii/S0731708509005123>>.
- <sup>10</sup>Ullman, Edwin F., et al. "Luminescent oxygen channeling immunoassay: Measurement of particle binding kinetics by chemiluminescence." *Proc Natl Acad Sci*. 91. (1994):5426-5430.  
<<http://www.pnas.org/content/91/12/5426.full.pdf>>.
- <sup>11</sup> Lakowicz, Joseph R.. *Principles of Fluorescence Spectroscopy*. 2<sup>nd</sup> ed. New York: Kluwer Academic/Plenum Publishers, 1999. Pg 367
- <sup>12</sup>Hiller, Yaffa, et al. "Biotin Binding to Avidin: Oligosaccharide side chain not required for ligand association." *Biochem. J*. 248 (1987):167-171.  
<<http://www.ncbi.nlm.nih.gov/pmc/articles/PMC1148514/pdf/biochemj00243-0162.pdf>>.
- <sup>13</sup> Hsu, Su-Ming, et al. "Use of avidin-biotin-peroxidase complex (ABC) in immunoperoxidase techniques." *J Histochem Cytochem*. 4 (1981):577-580.  
<<http://www.ncbi.nlm.nih.gov/pubmed/6166661>>.
- <sup>14</sup> Reichman, Jay. *Handbook of Optical Filters for Fluorescence Microscopy*. Chroma Technology Corp. 06/1998. <<http://depts.washington.edu/keck/handbook3.pdf>>.